

# Standardization of the Laser Notching Method for Measuring Fracture Toughness in Structural Ceramics

Anzhe Wang (✉ [wanganzhe14b@126.com](mailto:wanganzhe14b@126.com))

Nanjing Institute of Technology

Xinyuan Zhao

NJIT: Nanjing Institute of Technology

Mingxu Huang

NJIT: Nanjing Institute of Technology

Yehong Cheng

Hebei University of Technology

Dongyang Zhang

Sun Yat-Sen University

---

## Research Article

**Keywords:** Fracture toughness, Structural ceramics, Notch tip radius, Notch depth, Equivalent notch angle

**Posted Date:** January 25th, 2021

**DOI:** <https://doi.org/10.21203/rs.3.rs-152425/v1>

**License:** © ⓘ This work is licensed under a Creative Commons Attribution 4.0 International License.

[Read Full License](#)

---

# Standardization of the laser notching method for measuring fracture toughness in structural ceramics

Anzhe Wang<sup>1\*a,b</sup>, Xinyuan Zhao<sup>a</sup>, Mingxu Huang<sup>a</sup>, Yehong Cheng<sup>\*c</sup>, Dongyang  
Zhang<sup>\*d</sup>

<sup>a</sup> School of Materials Science and Engineering, Nanjing Institute of Technology,  
Nanjing 211167, P. R. China

<sup>b</sup> Jiangsu Key Laboratory of Advanced Structural Materials and Application  
Technology, Nanjing 211167, P. R. China

<sup>c</sup> School of Mechanical Engineering, Hebei University of Technology, Tianjin 300401,  
P. R. China

<sup>d</sup> School of Materials, Sun Yat-sen University, Guangzhou 510275, P. R. China

## Abstract

The single-edge V-notched beam (SEVNB) method based on the laser notching approach can effectively overcome the shortcoming of time-consuming and avoid large errors in traditional fracture toughness measurement ways, nevertheless the laser notching method has not yet been standardized. Taking oxide ( $ZrO_2$  and  $Al_2O_3$ ), carbide (SiC), nitride ( $Si_3N_4$ ) and boride ( $ZrB_2$ -based) ceramics as the research objects, this paper systematically discussed the effects of notch tip sharpness, notch depth and equivalent notch angle on the measured value of fracture toughness, thereby clearly defined the range of these parameters that required for measuring the fracture toughness accurately. Furthermore, in order to give full play to the advantages of the laser notching method, the feasibility of sample miniaturization was also discussed. This study could provide important data reference and theoretical basis for the standardization of laser method in the near future.

**Keywords:** Fracture toughness; Structural ceramics; Notch tip radius; Notch depth; Equivalent notch angle

---

*Corresponding author:* Tel/fax: +86 025 86118275

E-mail address: [wanganzhe14b@126.com](mailto:wanganzhe14b@126.com) (A.Z. Wang), [chengyehong@hebut.edu.cn](mailto:chengyehong@hebut.edu.cn) (Y.H. Cheng), [zhangdy58@mail.sysu.edu.cn](mailto:zhangdy58@mail.sysu.edu.cn) (D.Y. Zhang)

## 1. Introduction

Fracture toughness is one of the key and intrinsic material properties that is known as the critical stress intensity factor ( $K_c$ ) [1]. As ceramics mostly fail in mode I, which is the most common mode for laboratory testing, the  $K_c$  in mode I is referred to as  $K_{Ic}$ , which represents the fracture toughness corresponding to how much energy a material can absorb before catastrophic failure occurs under this mode. Accurate measurement of  $K_{Ic}$  is thus of great significance for the design, material selection and reliability evaluation of ceramic materials [2].

Under the unremitting efforts of scientists, numerous of standards for fracture toughness tests have been implemented worldwide, such as ASTM C1421-16 [3], ASTM E1820-13 [4], ASTM E1290-08 [5], ISO 15732-2003 [6], ISO 24370-2005 [7], ISO 23146-2012 [8], GB/T 23806-2009 [9] and DIN EN 14425-3 [10]. The recommended test methods in each standard are different, mainly including: single-edge V-notched beam (SEVNB) [11], single-edge precracked beam (SEPB) [12], chevron notch beam (CNB) [13], surface crack in flexure (SCF) [14], crack-tip opening displacement (CTOD) [15] methods, etc., as shown in Table 1.

Despite there is a wide range of methods to evaluate a ceramic's fracture toughness and the selection can be material and resource dependent, each one has obvious shortcoming. The SCF test needs fractographic expertise and careful grinding to remove residual stress, thus leading to a high randomness in its results [16]. The CNB method is generally preferred over the SCF method because it produces more consistent results if the notches are properly fabricated. However, the notch formation is difficult, which requires special machining fixture, and the stable crack growth in the notch plane is hard to detect [17]. The disadvantage of the CTOD specimen is that it is costly and difficult to machining owing to its relatively large and complex geometries [18]. SEPB method overcomes the drawback of single-edge notched beam (SENB) method, but the reliable introduction of a real crack into the ceramic sample is very difficult and the crack depth is uncontrollable [19,20].

By contrast, SEVNB, as an alternative to SEPB, is essentially a derivative of SENB method, replacing real crack with sharp V-shaped notches, which is an

convenient and frequently used method. Meanwhile, it has been recognized as having great advantages in specimen preparation, testing process, data accuracy, consistency, and reproducibility. In addition, SEVNB test procedure could also be easily modified toward the assessment of fracture toughness under shear loading via placing an eccentric notch on a testing specimen [17,21].

**Table 1** Advantages and disadvantages of using fracture toughness methodologies in various testing standards

| Testing standards | Areas         | Method | Advantages   | Disadvantages   |
|-------------------|---------------|--------|--|---|
| ISO 23146-2012    | International | SEVNB  | <ul style="list-style-type: none"> <li>• Relatively easy specimen fabrication</li> <li>• Low cost fixture</li> </ul>   | <ul style="list-style-type: none"> <li>• Difficult to achieve adequate V-notch fabrication</li> </ul>   |
| ASTM E1820-13     | USA           | SEVNB  | <ul style="list-style-type: none"> <li>• Does not require advanced fractography skills</li> </ul>  |   |
|                   |               | CTOD   | <ul style="list-style-type: none"> <li>• A relatively long crack length is available and relatively stable crack extension occurs under displacement controlled loading using a high stiffness testing machine which is ideal for subcritical crack growth and R-curve measurements</li> </ul> | <ul style="list-style-type: none"> <li>• A relatively complex specimen geometry which makes machining difficult and costly</li> <li>• The delicate precracking procedure, where some type of crack arrestor attachment is required for most brittle ceramics</li> </ul>           |
| ASTM E1290-08     | USA           | CTOD   |  |   |
| DIN EN 14425-3    | Germany       | CNB    | <ul style="list-style-type: none"> <li>• Not necessary to measure a precrack</li> </ul>  | <ul style="list-style-type: none"> <li>• Notch formation is difficult</li> <li>• Needs special machining fixtures</li> <li>• Requires stable crack growth in the notch and stable crack growth may be difficult to detect</li> <li>• Crack needs to follow notch plane</li> </ul> |
| ISO 24370-2005    | International | CNB    |  |   |
|                   |               | CNB    |  |   |
|                   |               | SCF    | <ul style="list-style-type: none"> <li>• Sharp and clinically-sized precracks</li> <li>• R-curve sensitive</li> </ul>  | <ul style="list-style-type: none"> <li>• Needs fractographic expertise</li> <li>• Careful grinding to remove residual stress</li> <li>• Needs mirror polished surface</li> </ul>  |
|                   |               | SEPB   | <ul style="list-style-type: none"> <li>• Produces sharp precracks</li> <li>• R-curve sensitive</li> </ul>  | <ul style="list-style-type: none"> <li>• Very difficult to produce real precrack (involves additional fixture and crack detection)</li> </ul>   |
| ISO 15732-2003    | International | SEPB   |  |   |
| GB/T 23806-2009   | China         | SEPB   |  |   |

It is noteworthy that preparing sharp enough V-notches on ceramic specimens is the prerequisite and also the difficulty for reliable fracture toughness assessment in SEVNB test. As we all know, apparent  $K_{Ic}$  values that are calculated from the maximum loads decrease with decreasing notch radius until some critical notch tip radius  $\rho_c$ , and the apparent  $K_{Ic}$  eventually become constant at the true value [18]. The  $\rho_c$  has been evident that is strongly dependent on the microstructure of the material.

However, there is no universal standard to determine the  $\rho_c$  value. Generally, the V-notch tip radius ( $\rho$ ) should satisfy the condition that the  $\rho$  is less than three times the average grain size in order to obtain the actual fracture toughness value [22]. For example,  $\rho_c$  value of very fine-grained yttria-stabilized tetragonal zirconia polycrystal (Y-TZP) ceramic with an average grain size of 0.5  $\mu\text{m}$  appears to be about or even less than 1.5  $\mu\text{m}$ , which in turn gives the theoretical upper limit of the sharp V-notch. Further clarification of the relationship between  $\rho_c$  and other microstructure characteristics of ceramics will help improve the measurement effectiveness of the SEVNB method.

In the last few decades, V-notch was often introduced by micro-milling [23] and/or razor blade sliding [22,24,25]. It is not only a time-consuming procedure, but also uncontrollable in keeping the same V-notch tip radius on both sides of the test specimens. More importantly, fabricating a sharp V-notch with the tip radius less than 5~10  $\mu\text{m}$  still remains a difficult task. Even if a sharp V-notch is finally acquired, the 5  $\mu\text{m}$  radius may still be insufficient for measuring the fracture toughness of fine ceramics, so that an overestimation of fracture toughness would come up due to the notch passivation effect [26].

Recently, laser micromachining techniques (including nanosecond laser [26], picosecond laser [27] and femtosecond laser [28-30]) have aroused scholars' great interests due to its high machining accuracy as well as efficiency, and have been successfully utilized to introduce sharp V-notches with tip radius less than 1  $\mu\text{m}$  (0.5  $\mu\text{m}$  [26,28] and 0.8  $\mu\text{m}$  [23]) in various materials (e.g.  $\text{ZrO}_2$ ,  $\text{Si}_3\text{N}_4$ ,  $\text{ZrB}_2$ -SiC, etc.) so far. Although the laser method will inevitably lead to physical changes of the material (such as remelting and recrystallization), several previous studies have shown that the molten zone at the V-notch tip is generally less than 2  $\mu\text{m}$ , which is ignorable during fracture toughness tests [31,32]. Furthermore, Zhao *et al.* [33] have revealed that the effect of thermal stresses induced by laser can also be ignored after comparing the fracture toughness value of the fine-grained alumina before and after annealing. Apart from these, the laser method has many other exciting advantages: (i) excellent efficiency (sharp V-notches are easy to prepare and only takes a few seconds); (ii) flat

bottom of the V-notch and good consistency of the notch depth on both sides of the sample and (iii) the plane of the final crack measured from the tip of the V-notch always parallel to both the test specimen dimensions width and thickness within 5°. Based on these significant advantages, many scholars have pointed out that the laser method is a very promising standardized method for measuring fracture toughness.

At present, there are still many challenges in the popularization and application of laser method, including: (i) laser notching is generally based on experience, while lack of available criteria to point out how sharp the V-notches should be for different ceramics with various compositions and microstructures; (ii) based on the current test standards, the notch depth should be in the order of millimeters, far beyond the laser notching depth (tens to hundreds of microns). Therefore, the laser method should be utilized in combination with the traditional methods, which leads to an equivalent notch angle in the compound notch (U-groove+V-notch) [11]. It is urgent to clarify the reasonable range of equivalent notch angle, that is, to define the relationship between the V-notch depth and the U-groove width; (iii) it is essential to fully understand the relationship between relative notch depth (notch depth/sample thickness) and the fracture toughness measurement values of different ceramics, so as to formulate the reasonable notch depth range; and (iv) the corresponding improvement of specimen size, especially the feasibility of small and thin specimens.

In response to the above problems, taking a variety of typical structural ceramics (including commercial 5Y-TZP, Si<sub>3</sub>N<sub>4</sub>, SiC and Al<sub>2</sub>O<sub>3</sub> ceramics as well as self-prepared ZrB<sub>2</sub>-based ceramics) as the study objects, the relationship between fracture toughness measurement values and notch tip radius, notch depth, equivalent notch angle as well as sample size were systematically studied.

## **2. Experimental procedures**

### **2.1 Material and test samples**

5 mol% yttria-stabilized tetragonal zirconia polycrystal (5Y-TZP), SiC and Al<sub>2</sub>O<sub>3</sub> ceramics were provided by Zhuhai Jiawei Ceramic Technology CO., LTD. Si<sub>3</sub>N<sub>4</sub> ceramics were purchased both from Zhuhai Jiawei Ceramic Technology CO., LTD. and Zhuhai Yuebojia New Material CO., LTD., and we name it Si<sub>3</sub>N<sub>4</sub>(J) and Si<sub>3</sub>N<sub>4</sub>(Y),

respectively.  $ZrB_2$ ,  $ZrB_2$ -20 vol.% SiC ( $ZrB_2$ -SiC) and  $ZrB_2$ -20 vol.% SiC-15vol.% Graphite ( $ZrB_2$ -SiC-Graphite) ceramics were fabricated by hot-pressing method, and the detailed preparation procedures were described in our previous article [26]. Substrates were cut into the test pieces with the size of  $2 \times 4 \times 22 \text{ mm}^3$  and  $3 \times 4 \times 40 \text{ mm}^3$  in accordance with ASTM E1820-13 [4] and ISO 15732-2003/GB/T 23806 [6,9], respectively, to study the effects of notch tip radius, notch depth and equivalent notch angle on the measured fracture toughness value. Moreover, non-standard samples with the sizes of  $2 \times 1 \times 16 \text{ mm}^3$  and  $2 \times 2 \times 16 \text{ mm}^3$  were also prepared from the same bulk for the comparison of the sample size effect. The fracture surfaces of all specimens were checked by the scanning electron microscopy (SEM, Merlin Compact, Carl Zeiss AG), and the micrographs are shown in Fig. 1.

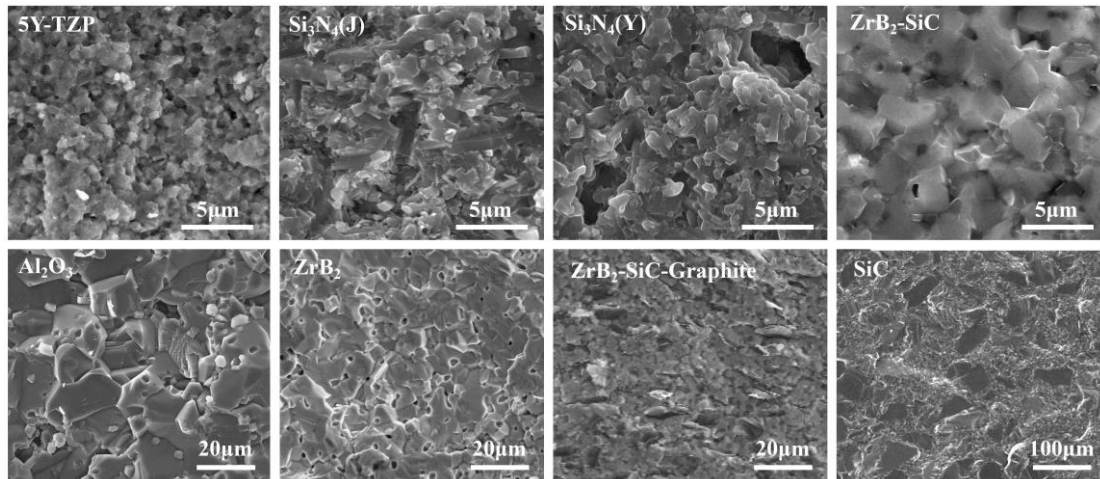


Fig. 1. SEM images of fracture surfaces of test samples.

## 2.2 Notching methods

U-grooves with different widths and depths on the  $B \times S_0$  surfaces in non-conductive (5Y-TZP,  $Si_3N_4(J)$ ,  $Si_3N_4(Y)$ , SiC and  $Al_2O_3$ ) and conductive ( $ZrB_2$ ,  $ZrB_2$ -SiC and  $ZrB_2$ -SiC-Graphite) ceramic samples were fabricated using diamond wheels and wire cutting machine, respectively. To get sharper notches with different tip radius, V-notches were polished along the prefabricated U-grooves using razor blades sprinkled with the 1 to 20  $\mu\text{m}$  diamond pastes. However, the notch tip radius ( $\rho$ ) prepared by the above-mentioned traditional methods was difficult to reach 10  $\mu\text{m}$ .

In order to introduce sharper V-notches, here, nanosecond laser (DX-FM20, Nanjing Dingxin Electromechanical Equipment Co., Ltd., China) with the wavelength

of 1064 nm, pulse width of 10 ns, power of 1-20 W and scan speed of 10-50 mm·s<sup>-1</sup> was used for multiple processing on the center of the surfaces in test bars. Typical sharp notch on ceramic sample is presented in Fig. 2. By adjusting the laser notching parameters, i.e., power, scan speed and notching times, sharp V-notches with different depths (ranging from 10 to 500 μm) could be achieved. For deeper notches, laser method could be utilized in conjunction with traditional notching method, see Fig. 3. In this case, it should be noted that the equivalent notch angle ( $\theta$ ) will change with the width of the U-groove and the depth of the V-notch.

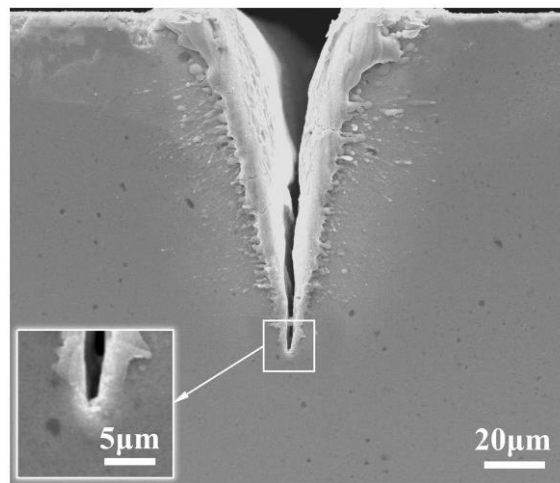


Fig. 2. SEM image of 5Y-TZP ceramic bar with an ultra-sharp V-notch. The enlarged view shows that the V-notch tip radius is  $\sim 0.7 \mu\text{m}$  and no microcrack is found near the V-notch root.

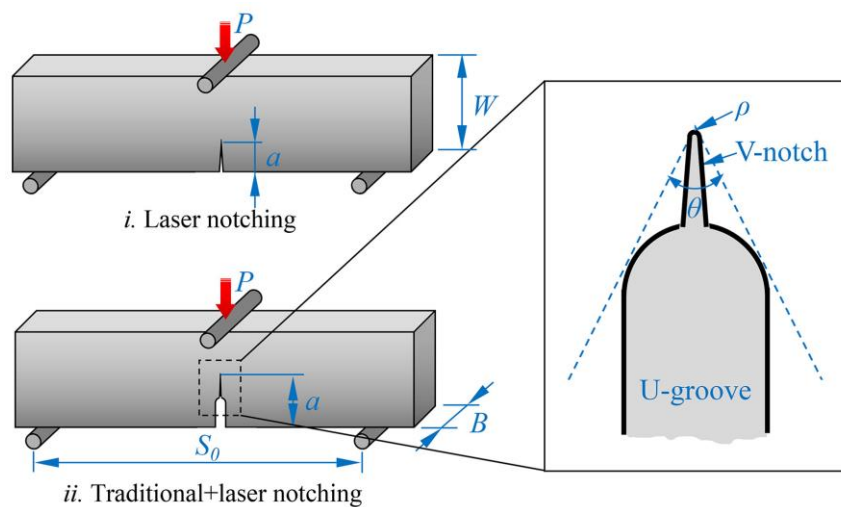


Fig. 3. Schematic of the SEVNB test specimens with sharp notches.

### 2.3 Fracture toughness tests

Fracture toughness was determined by the three-point SEVNB method (SFL-50KNAG, SHIMADZU, China) with a cross head speed of 0.05 mm·min<sup>-1</sup>. The fracture toughness ( $K_{Ic}$ ) of standard-sized specimens were calculated with reference to the corresponding standards [4,6], while the  $K_{Ic}$  value of non-standard samples were calculated by using the following expression [34]:

$$K_{Ic} = \frac{3P_{\max}S_0}{2BW^2} Y \sqrt{a} \quad (1)$$

$$Y = \frac{1.1215\sqrt{\pi}}{\beta^{3/2}} \left[ \frac{5}{8} - \frac{5}{12}\alpha + \frac{1}{8}\alpha^2\beta^6 + \frac{3}{8}\exp\left(-\frac{6.1342\alpha}{\beta}\right) \right] \quad (2)$$

where  $P_{\max}$  is the fracture load;  $S_0$  is the span width;  $B$  is the sample width;  $W$  is the sample height;  $a$  is the notch depth;  $\alpha$  is the relative notch depth defined by  $a/W$  and  $\beta = 1-\alpha$ . All of the notch depths were carefully measured by SEM examinations of the fractured cross sections of the specimens.

### 3. Results and discussion

#### 3.1 Effect of notch tip radius

According to the Griffith's theory, the critical stress intensity factor ( $K_c$ ) remains unchanged, which can be regarded as the fracture toughness ( $K_{Ic}$ ), when  $\rho$  is within the critical value ( $\rho_c$ ), and is proportional to  $\rho^{0.5}$  when  $\rho$  exceeds the threshold level, as shown by the gray dotted line in Fig. 4a. However, it exhibits different degrees of error on this criterion for different ceramics, which is reflected in the change of slope [26]. To thoroughly understand the relationship between  $K_c$  and  $\rho$ , the experimental data were analyzed in double logarithmic coordinates, and the data in the literature were redrawn at the same time for comparison, as depicted in Fig. 4b-f. The apparent  $K_{Ic}$  values of the fifteen kinds of ceramics increase linearly with the notch tip radius when  $\rho > \rho_c$ . Linear regression is used to obtain the best fit for the data and the slope is in the range of 0.1-0.5. This indicates that the fracture toughness ( $K_{Ic}$ ) of structural ceramics is proportional to  $\rho^n$ , where  $n$  is normally less than 0.5 and strongly depends on the material itself. The greater the value of  $n$ , the more sensitive the material to the notch tip radius. Furthermore, a blunt notch may cause some errors in the comparison of  $K_{Ic}$  between different kinds of materials. For example, the  $K_{Ic}$  of Al<sub>2</sub>O<sub>3</sub>(T) is larger

than that of  $\text{Al}_2\text{O}_3(\text{B})$  in the case of  $\rho < 200 \mu\text{m}$ , while a contrary result is obtained when  $\rho > 200 \mu\text{m}$ , as can be seen in Fig. 4f. Similar results can also be detected when comparing  $\text{ZrB}_2\text{-SiC}$  with  $\text{ZrB}_2\text{-SiC-Graphite}$  ceramics [26].

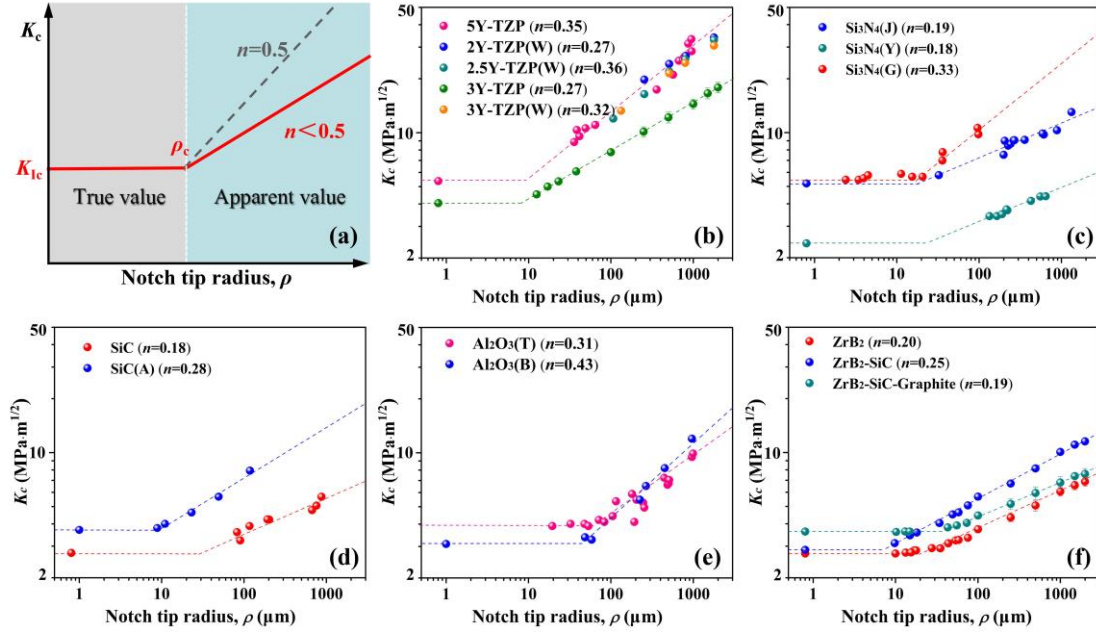


Fig. 4. Variation of the critical stress intensity factor ( $K_c$ ) with notch tip radius ( $\rho$ ). (a) Schematic diagram and test results of (b) yttria-stabilized zirconia, (c) silicon nitride, (d) silicon carbide, (e) alumina as well as (f)  $\text{ZrB}_2$ -based ceramics in double logarithmic coordinates.

In the measurement of fracture toughness via SEVNB method, the relationship between  $K_c$ ,  $\rho_c$  and  $n$  value is very noticeable: (i) For the same type of material, the fracture toughness is not necessarily related to the slope or the critical notch tip radius. The slope of 0.28 in  $\text{SiC}(\text{A})$  ceramic with high fracture toughness ( $3.70 \text{ MPa}\cdot\text{m}^{1/2}$ ) is higher than that of  $\text{SiC}$  with relative low fracture toughness, but the  $\rho_c$  of  $\text{SiC}(\text{A})$ , less than  $10 \mu\text{m}$ , is only  $\sim 1/3$  of that of  $\text{SiC}$ , as illustrated in Fig. 4d and Table 2, which means that the V-notch required for the accurate measurement of fracture toughness in  $\text{SiC}(\text{A})$  is sharper. On the contrary, alumina with high fracture toughness corresponds to a lower slope ( $n$ ) and a higher critical notch tip radius ( $\rho_c$ ), see Fig. 4e. (ii) For materials with similar  $\rho_c$  and  $n$  values, the difference in fracture toughness values may also be significant. For example, in Fig. 4c, even though the  $\rho_c$  and  $n$  of  $\text{Si}_3\text{N}_4(\text{J})$  and  $\text{Si}_3\text{N}_4(\text{Y})$  are almost the same as  $\sim 20 \mu\text{m}$  and  $\sim 0.18$ , respectively, the fracture

toughness values of the two are more than doubled (5.20 and 2.41 MPa·m<sup>1/2</sup>, respectively). (iii) Even though the fracture toughness are similar, the material's sensitivity to the notch may vary greatly, which reflected in the notable difference of slope  $n$ , such as Si<sub>3</sub>N<sub>4</sub>(J) and Si<sub>3</sub>N<sub>4</sub>(G), the fracture toughness of the former are close to that of the latter (~5 MPa·m<sup>1/2</sup>), but the notch sensitivity and the  $n$  value of Si<sub>3</sub>N<sub>4</sub>(J) decrease obviously which may owing to the whisker toughening by rod-like silicon nitride, as depicted in Fig. 2.

Although the relationship between the  $K_c$ ,  $\rho_c$  and  $n$  value is very complicated, the most important concern is how sharp the V-notch tip radius ( $\rho$ ) is enough to obtain the actual fracture toughness value. It is generally accepted that  $\rho_c$  seems to be strongly dependent on the microstructure of the material [18,35], and the previous theoretical calculation formulas can be expressed as:

$$\rho_c \approx \frac{4Y_0^2}{[\tanh^{-1} X]^2} \delta a \quad (3)$$

in Damani model [36] and

$$\rho_c = \left[ \frac{x^* K_{Ic}^2}{8.8E\sigma_Y \varepsilon_f(R_\beta)} \right]^{1/2} \quad (4)$$

in Malkin model [37], respectively, where  $\delta a$  is the size of the flaw that caused the fracture initiation,  $Y_0$  is 1.12 for a through-thickness edge crack,  $X$  is between 0.9 and 0.95,  $K_{Ic}$  is fracture toughness,  $\sigma_Y$  is yield strength in tension,  $E$  is elastic modulus,  $x^*$  is the size of the constant strain zone at the notch root, and  $\varepsilon_f(R_\beta)$  is tensile fracture strain. In Eq. (3), the notch-tip small cracks are assumed to be related to some characteristic feature of the microstructure so  $\delta a$  is depended on the basis of microstructural studies. However, no obvious suitable microstructural feature is found at present. In Eq. (4), the accuracy of the  $\rho_c$  and  $K_{Ic}$  values are interdependent and the  $x^*$  value that describes the microscopic properties of the material is very difficult to obtain.

In view of these limitations, experimental estimation of the  $\rho_c$  in ceramic is more popular. Previous studies have pointed out that the  $\rho_c$  is positively correlated with the average grain size ( $d_{50}$ ) and appears to be less than 10  $\mu\text{m}$  for some fine grain size

ceramics [18], such as polycrystalline alumina ( $d_{50}$  is  $\sim 1 \mu\text{m}$  and  $\rho_c$  is  $\sim 9 \mu\text{m}$ ) [38], zirconia ( $d_{50} < 1 \mu\text{m}$  and  $\rho_c < 10 \mu\text{m}$ ) [36] and hot-pressed silicon nitride ( $d_{50} < 3 \mu\text{m}$  and  $\rho_c < 15 \mu\text{m}$ ) [36]. Some scholars believe that the  $\rho$  should comply with the condition that the  $\rho$  should be less than three times the average grain size ( $3d$ ) [22], however, there is a lack of experimental verification. Here, the critical notch tip radius ( $\rho_c$ ) can be deduced according to the linear law in Fig. 4. It is found that  $3d$  is often much lower than the  $\rho_c$  for fine-grained ceramics (e.g.,  $\rho_c$  value of very fine-grained 5Y-TZP ceramic with an average grain size of  $0.5 \mu\text{m}$  appears to be about or even less than  $1.5 \mu\text{m}$ , much less than the critical value of  $9.41 \mu\text{m}$  obtained by experiments, see Table 2), and if the excessively strict notch sharpness requirements of  $3d$  are continued, it will be extremely difficult to introduce sharp enough notches into fine-grained ceramics, which are both hard and brittle, by traditional notching method.

As reported by Damani *et al.* [36], the magnitude of  $\rho_c$  is proportional to the size of the critical fracture-initiating flaw, corresponding to the the critical flaw size ( $a_c$ ), which reflects the sensitivity of the material to stress concentration. Here, we compared the  $a_c$  and the  $\rho_c$  subsequently, wherein the  $a_c$  of these ceramics were calculated by the following formula [39]:

$$a_c \approx K_{Ic}^2 / (\pi \sigma_0^2) \quad (5)$$

where  $\sigma_0$  is the original strength and the  $K_{Ic}$  value is obtained from sharp notched SEVNB method. As listed in Table 2 below, the  $a_c$  of most ceramics are very close to their  $\rho_c$ , while the  $a_c$  values of some ceramics with R-curve behaviour are even slightly lower than that of the  $\rho_c$ . For instance, ZrB<sub>2</sub>-SiC-G ceramic, which exhibits significant R-curve behavior caused by the graphite toughening phase, as reported in Ref. [40], has a larger  $\rho_c$  of  $36.17 \mu\text{m}$  than the  $a_c$  of  $25.56 \mu\text{m}$ . The  $\rho_c$  of  $45.43 \mu\text{m}$  for coarse-grained alumina, Al<sub>2</sub>O<sub>3</sub>(B), which could be accompanied by obvious crack propagation resistance [41], is also much greater than its  $a_c$  of  $24.97 \mu\text{m}$ . The above results are consistent with the results of Fett [42], which indicate that the existence of R-curve behaviour imply higher value of the critical notch tip radius required in SEVNB specimens for a reliable assessment of the fracture toughness.

Therefore, regardless of whether the ceramic has R-curve characteristics,  $a_c$  can be regarded as a new criterion for making sharp notches, i.e., the accuracy of measured value of fracture toughness can be assured as long as the notch tip radius,  $\rho$ , is less than  $a_c$ . Although the calculation of  $a_c$  relies on the measurement of  $K_{Ic}$ , as can be seen in Eq. (5), the lower limit of the critical notch tip radius in ceramics,  $\rho_c$ , (corresponding to the  $a_c$ ) can be obtained through extreme case assumptions. Generally, the fracture toughness value of ceramics is not less than  $2 \text{ MPa}\cdot\text{m}^{1/2}$  [43], and the bending strength is difficult to exceed 1 GPa [44,45]. Thus, the minimum critical flaw size of existing ceramics can be estimated by  $2^2/(3.14\times 1000^2) \text{ m}\approx 1.27 \text{ }\mu\text{m}$ , which is slightly larger than the notch tip radius ( $< 1 \text{ }\mu\text{m}$ ) introduced by laser method. Ceramics with higher strength are often accompanied by greater fracture toughness, resulting in larger critical flaw size,  $a_c$ , and critical notch tip radius,  $\rho_c$  (for example, the strength of 2 GPa in ZrO<sub>2</sub>-WC nanocomposites corresponds to the  $K_{Ic}$  of  $9.4 \text{ MPa}\cdot\text{m}^{1/2}$  and the  $a_c$  value of  $7.04 \text{ }\mu\text{m}$  [46]). Malkin model is also used to assess the minimum  $\rho_c$  in ceramics. Taking  $K_{Ic}$  of  $2 \text{ MPa}\cdot\text{m}^{1/2}$  [43],  $\sigma_Y$  of 500 MPa [47],  $E$  of 541 GPa [48],  $x^*$  of  $1 \text{ }\mu\text{m}$  [36,37],  $\varepsilon_f(R_\beta)$  of 0.1% [49] as the limit values, the  $\rho_c$  calculated by Eq. (4) is  $1.30 \text{ }\mu\text{m}$ , which is consistent with the lower threshold value achieved by Eq. (5). Therefore, it could be reasonable to believe that the V-notch produced by laser notching method is sharp enough for all ceramics.

**Table 2** Material parameters and mechanical properties of sixteen kinds of ceramics

| Materials  | Original strength, $\sigma_0$ (MPa) | Fracture toughness, $K_{Ic}$ ( $\text{MPa}\cdot\text{m}^{1/2}$ ) | Three times the average grain size, $3d$ ( $\mu\text{m}$ ) | Critical flaw size, $a_c$ ( $\mu\text{m}$ ) | Critical notch tip radius, $\rho_c$ ( $\mu\text{m}$ ) | $n$ value |
|--|-------------------------------------|--|--|---|---|-----------|
| 5Y-TZP   | 913                                 | 5.37   | ~1.5   | 11.01                                       | ~9.41   | 0.35      |
| 2Y-TZP(W) <sup>[50]</sup>                          | 980                                 | -  | -  | -   | -   | 0.27      |
| 2.5Y-TZP(W) <sup>[50]</sup>                        | 870                                 | -  | -  | -   | -   | 0.36      |
| 3Y-TZP(W) <sup>[50]</sup>                          | 780                                 | -  | -  | -   | -   | 0.32      |
| 3Y-TZP <sup>[26]</sup>                             | 770                                 | 4.05   | ~1.5   | 8.81  | ~8.03   | 0.27      |
| Si <sub>3</sub> N <sub>4</sub> (J)                 | 664                                 | 5.20   | ~4.5   | 19.52                                       | ~18.55  | 0.19      |
| Si <sub>3</sub> N <sub>4</sub> (Y)                 | 283                                 | 2.41   | ~3.6   | 23.08                                       | ~23.43  | 0.18      |
| Si <sub>3</sub> N <sub>4</sub> (G) <sup>[51]</sup> | 700                                 | 5.40   | ~12  | 18.94                                       | 17.72   | 0.33      |
| SiC  | 305                                 | 2.75   | ~18  | 25.88                                       | ~27.99  | 0.18      |
| SiC(A) <sup>[52]</sup>                             | 620                                 | 3.70   | -  | 11.34                                       | 9.5   | 0.28      |

|  |     |      |      |       |        |      |
|--|-----|------|------|-------|--------|------|
| Al <sub>2</sub> O <sub>3</sub>                     | 307 | 2.93 | ~30  | 28.99 | -      | -    |
| Al <sub>2</sub> O <sub>3</sub> (T) <sup>[53]</sup> | 297 | 3.80 | ~7.5 | 52.11 | 61.40  | 0.31 |
| Al <sub>2</sub> O <sub>3</sub> (B) <sup>[54]</sup> | 350 | 3.10 | ~30  | 24.97 | 45.43  | 0.43 |
| ZrB <sub>2</sub>                                   | 456 | 2.73 | ~24  | 14.03 | ~18.88 | 0.20 |
| ZrB <sub>2</sub> -SiC                              | 740 | 2.86 | ~9   | 4.75  | ~7.45  | 0.25 |
| ZrB <sub>2</sub> -SiC-G                            | 404 | 3.62 | -    | 25.56 | ~36.17 | 0.19 |

### 3.2 Effect of notch depth

The critical stress intensity factor ( $K_c$ ) values of these typical structural ceramics which are measured by different notch depths are plotted in Fig. 5. It can be seen clearly that the  $K_c$  values obtained by SEVNB method are closely correlated with the  $a/W$ . In contrast to metals [55], the  $K_c$  values increase rapidly when  $a/W$  is below a critical value, which might be determined by material itself (i.e., the composition and the microstructure), and then remain constant at the fracture toughness ( $K_{Ic}$ ). This is consistent with the previous reports that the  $K_c$  of shallow notched brittle materials are lower than that for deep notches or large cracks [56].

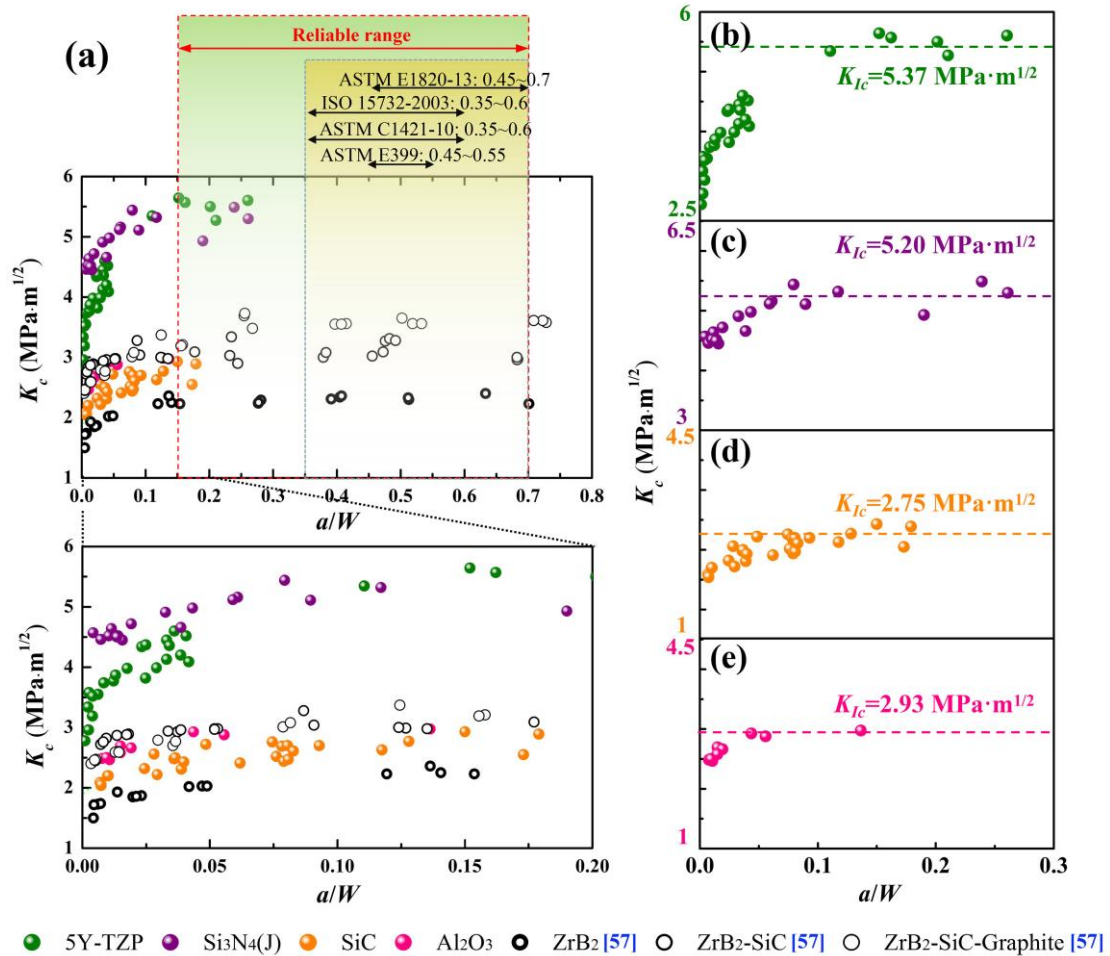


**Fig. 5.** Fracture toughness of various ceramics with different  $a/W$  measured by laser notched SEVNB method. (a) Our work and the literature report data [57] and (b) 5Y-TZP, (c)  $\text{Si}_3\text{N}_4(\text{J})$ , (d) SiC as well as (e)  $\text{Al}_2\text{O}_3$  ceramics, respectively.

The critical value of  $a/W$  is not more than 0.15 whether it is oxide, nitride, carbide or boride ceramics, and even for ceramic matrix composites containing a large amount of toughened phases (i.e., ZrB<sub>2</sub>-20 vol.% SiC-15vol.% Graphite), a relative depth  $a/W$  of 0.25 is also deep enough. Nevertheless, current commonly used test standards prescribe that the  $a/W$  should be between 0.35 and 0.7, and the ASTM E399 even requires the relative depth ranging from 0.45 to 0.55. Obviously, the  $a/W$  requirement in current standards seem to be too harsh, this may be because: (i) In the past, it is tough to introduce shallow notches (less than 1 mm) into ceramics because the traditional notching methods are difficult to control the notch depth; (ii) Making a notch with uniform depth is not trivial, and this will be more difficult especially when the notch is shallow, which in turn leads to large errors in fracture toughness measurements.

By observing the cross-sectional morphology of the ceramic specimens processed by the novel laser notching method, it is found that the notch depth is very uniform (i.e., the depth deviation in 5Y-TZP ceramic does not exceed 8%, and the maximum and minimum depths are 76  $\mu\text{m}$  and 70  $\mu\text{m}$ , respectively, as drawn in Fig. 6), which indicates that the above-mentioned problems could be effectively solved by the laser method. Through adjusting the laser processing parameters, it is clear that the notch bottom is flat at various notch depths (see Fig. 7a-c), while the roughness at the bottom increases slightly with increasing notch depth. In the view of the large enough notch depth, the deviation of the  $a/W$  will not increase significantly and thus the error of the notch depth could be neglected. Furthermore, partially enlarged view indicates that there is no remelting, recrystallization, microcrack or other damages near the notching boundary (as shown in Fig. 7d and e). In the past, Turon-Vinas *et al.* [58,59] observed a narrow microcracked region (damage zone) in front of the notch tip in ceramics after laser processing. Subsequently, Zhao *et al.* [31] revealed that the

damage zone in front of V-notch tip was just superficial and could be easily removed by polishing. In addition, based on the fracture analysis and comparison of the measured values before and after acidic pickling (hydrofluoric acid) as well as annealing for  $\text{Si}_3\text{N}_4$  [31], 3Y-TZP [32],  $\text{Al}_2\text{O}_3$  [32,33] and 8Y-FSZ [32] ceramics, they further proved that the effect of the physical changes of the material (such as remelting and recrystallization) and the residual thermal stress on the fracture toughness measurement results could be ignored. Our previous researches also excluded the influence of laser processing residual stress [11,26,57]. In view of this, we believe that the appropriate nanosecond laser processing has only a minimal/negligible effect on the microstructure of the material, thus achieving the true fracture toughness in ceramics during SEVNB test.

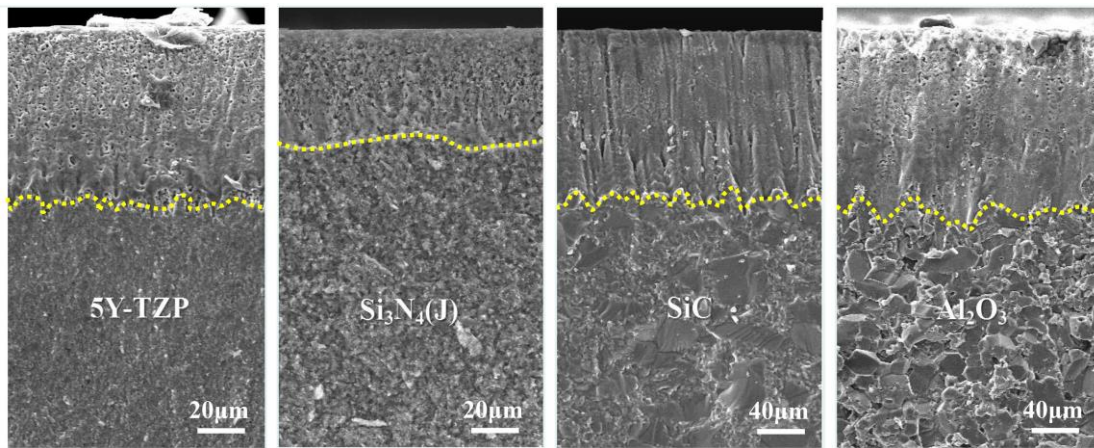


Fig. 6. Fracture surfaces of test ceramics notched by nanosecond laser.

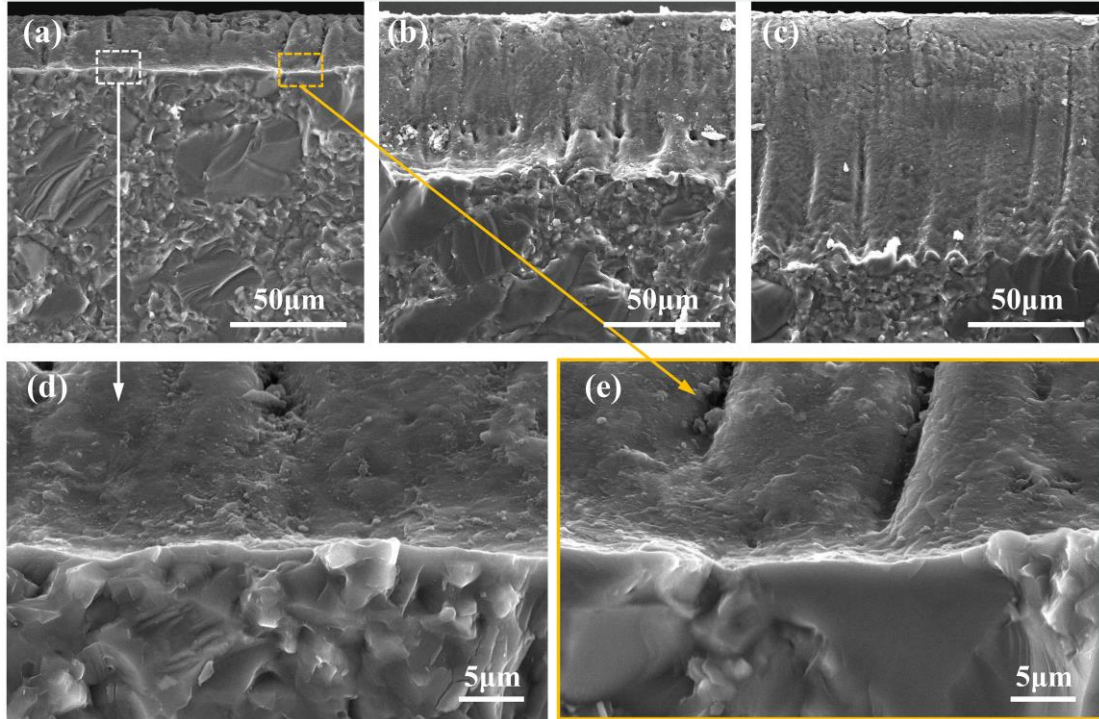


Fig. 7. Fracture surfaces of SiC ceramic with various notch depth.

Since the fracture toughness is calculated by fracture strength ( $\sigma$ ) as well as relative depth ( $a/W$ ) values, if the relationship between  $\sigma$  and notch depth ( $a$ ) or  $a/W$  are well established, the fracture toughness measurement could be guided more effectively. As depicted in Fig. 8, the experimental data of  $\sigma$  vs  $a$  was analyzed in double logarithmic coordinates based on the linear elastic fracture mechanics (LEFM). The strength values of these ceramics decrease linearly with the notch depth, which is close to those previous studies of typical ceramics containing indentation [60,61] and femtosecond laser processing pore-like flaws [62]. Linear regression was then applied, and it is exciting that the slope value  $m$  proposed by LEFM is not constant at -0.5 but depending on material itself to a large extent ( $m$  is -0.383, -0.372, -0.381 and -0.395 for 5Y-TZP, Si<sub>3</sub>N<sub>4</sub>(J), SiC and Al<sub>2</sub>O<sub>3</sub> ceramics, respectively).

In theory, a flaw-free sample should be able to sustain a mechanical stress near the theoretical strength ( $\sigma_{th}$ ) of solid. Thus, linear extrapolations to very shallow notch sizes (atomic scale,  $\sim 3 \text{ \AA}$  in Ref. [63]) were put into effect, and the estimated ultimate strength ( $\sigma_{max}$ ) is about 20.9, 30.8, 17.4 and 22.0 GPa for 5Y-TZP, Si<sub>3</sub>N<sub>4</sub>(J), SiC and Al<sub>2</sub>O<sub>3</sub> ceramics, respectively. Rely on the relationship between theoretical strength and elastic modulus ( $\sigma_{th}$  is in the order of  $\sim E/10$  to  $E/30$  in Ref. [64]), and by applying

the elastic modulus values as reported in Refs. [65-68], we can estimate that the  $\sigma_{th}$  is 7.7-23.0, 11.2-33.5, 11.7-35.0 and 13.3-40.0 GPa for 5Y-TZP, Si<sub>3</sub>N<sub>4</sub>(J), SiC and Al<sub>2</sub>O<sub>3</sub> ceramics, respectively. It is exciting that the theoretical  $\sigma_{max}$  values for these four typical structural ceramics obtained by linear extrapolation are in good agreement with the  $\sigma_{th}$  values. Similar phenomenon has also been revealed in boride ceramics [57]. In light of the above-mentioned exponential relationship between fracture strength ( $\sigma$ ) and notch depth ( $a$ ), it can be used not only to predict the theoretical strength ( $\sigma_{th}$ ) of ceramics, but also to deduce the  $\sigma$  value at different  $a$  when the  $\sigma_{th}$  is known (such as first-principles calculations [69]), so as to obtain the relationship between critical stress intensity factor ( $K_{Ic}$ ) and  $a$  according to the fracture toughness calculation formula.

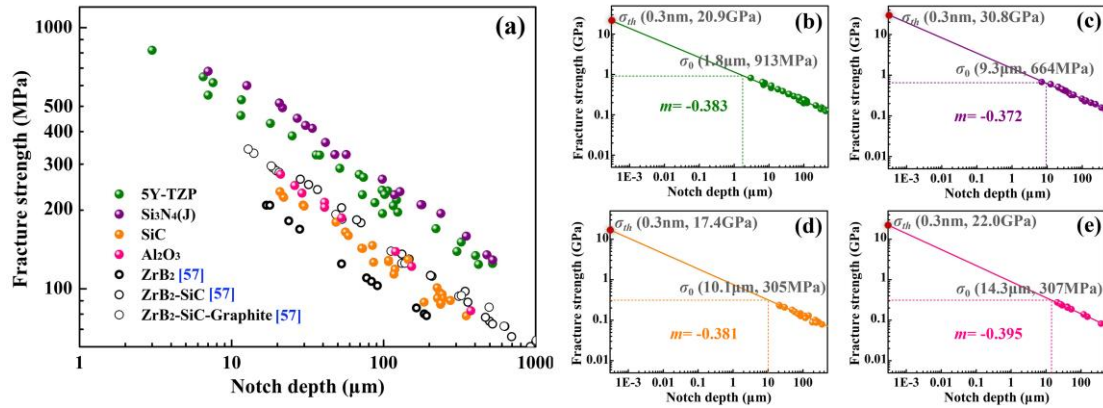


Fig. 8. Relationship between fracture strength and notch depth for various ceramics in double logarithmic coordinates. (a) Our work and the literature report data [57] and (b) 5Y-TZP, (c) Si<sub>3</sub>N<sub>4</sub>(J), (d) SiC as well as (e) Al<sub>2</sub>O<sub>3</sub> ceramics, respectively.

### 3.3 Effect of equivalent notch angle

To the author's best knowledge, the laser notch depth is often less than 500  $\mu\text{m}$  (even laborious to achieve 100  $\mu\text{m}$  via the femtosecond laser as reported in Refs. [28,58]), which is far less than the depth of at least 1 mm that recommended in test standards. Thus, the laser notching approaches should be utilized in combination with the traditional U-groove notching methods, resulting in an equivalent notch angle ( $\theta$ ) which is determined by the laser notch depth and the U-groove width. Here, the measured values of fracture toughness ( $K_{Ic}$ ) at different  $\theta$  are plotted in Fig. 9. It is obvious that when  $\theta$  is below about 60°, the  $K_{Ic}$  value stays almost constant at the

intrinsic value (or name it the actual value), and then increases gradually as the  $\theta$  increases. Similar to those reported by GÓMEZ [70] for some brittle or quasi-brittle materials with good processability, the approximate expression of the measured  $K_{Ic}$  value can be expressed as:

$$K_{Ic,measured} = [1 + 0.038393(\pi\theta/180)^2 - 0.027857(\pi\theta/180)^3 + 0.024207(\pi\theta/180)^4] \cdot K_{Ic,actual} \quad (6)$$

where  $K_{Ic,actual}$  is obtained by sharp V-notches,  $\theta$  ranges from  $0^\circ$  to  $160^\circ$ .

It can be seen that the experimental results agree well with the predicted values (solid lines in Fig. 9). From the predicted curves, it is clear that the  $K_{Ic,measured}$  could be regarded as being accurate when the  $\theta$  is less than  $60^\circ$ . However, there is an inevitable deviation between the center lines of the laser V-notch and the U-groove during notching process, which in turn leads to the measurement errors of  $K_{Ic}$ . For instance, the  $\theta$  of the two typical notches of 5Y-TZP ceramic are basically the same as  $65^\circ$  and  $67^\circ$ , see Fig. 9a, respectively, wherein the former is almost symmetrical along the notch centerline and the error between the experimental as well as the prediction results is less than 3%, while a 10% mistake is exhibited in the latter one, which may owing to the 0.09 mm deviation between the laser V-notch and the U-groove. It is not trivial to control the position of the V-notch on most commercial lasers equipment, especially on the order of 0.1mm, thus, in order to accurately measure the fracture toughness, the  $\theta$  should be small enough, which requires reducing the U-groove width and increasing V-notch depth as much as possible. At present, the  $\theta$  recommended by ASTM E1820-13 [4] and ISO 23146-2012 [8] are  $60^\circ$  and  $30^\circ$ , respectively, and the latter standard would be more conducive to obtaining the accurate fracture toughness value.

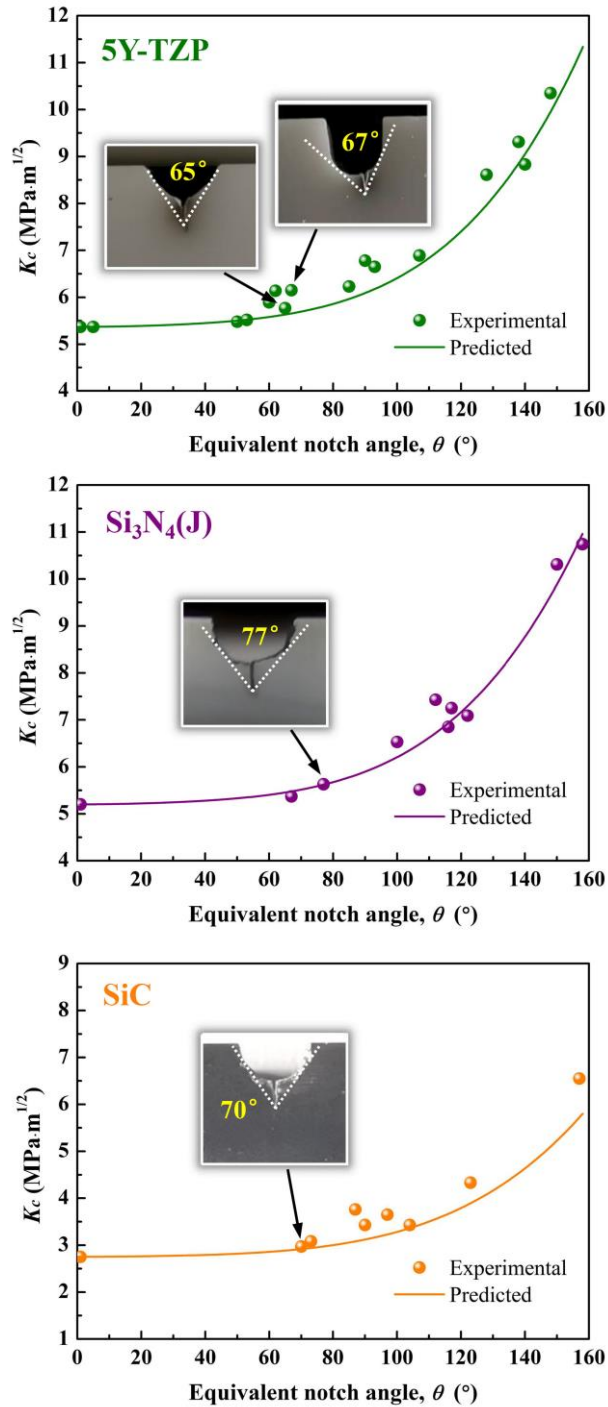


Fig. 9. Experimental and predicted values of  $K_c$  in 5Y-TZP,  $\text{Si}_3\text{N}_4(\text{J})$  and SiC samples with various equivalent notch angles ( $\theta$ ).

### 3.4 Effect of sample size

In order to meet the current standards, it is unavoidable to perform a traditional notching process before laser notching, which restricts the important advantages of laser method as simple and efficient. If a thinner specimen is used, only the laser

notching approach is required to achieve a sharp V-notch with satisfactory sharpness ( $\rho < 1 \mu\text{m}$ ), sufficient relative notch depth ( $a/W > 0.15$ ) and ideal equivalent notch angle ( $\theta < 10^\circ$ ). Here, smaller and thinner specimens were used for the SEVNB test, and the test results were compared with that of the current standards of ASTM E1820-13 [4] and GB/T 23806 [9], as plotted in Fig. 10. The small-sized sample test results of the five kinds of ceramics are in good agreement with the results of the standard samples (error does not exceed  $\pm 5\%$ ), indicating that the reduction in sample size will not affect the test accuracy. Miyazaki *et al.* [71] have also measured the fracture toughness of typical ceramics (including  $\text{Al}_2\text{O}_3$ ,  $\text{AlN}$  and  $\text{Si}_3\text{N}_4$ ) thin plates with thickness of 0.32 mm and 0.64 mm by means of several testing institutions, and a similar conclusion is given that the sample thickness has no effect on the measured value.

Therefore, using small and thin SEVNB samples could give full play to the advantages of laser notching method without reducing the test accuracy, especially in the case of limited billet or substrate in the development of new materials, it can replace the indentation method, which often comes at the cost of losing part of the test precision and reliability.

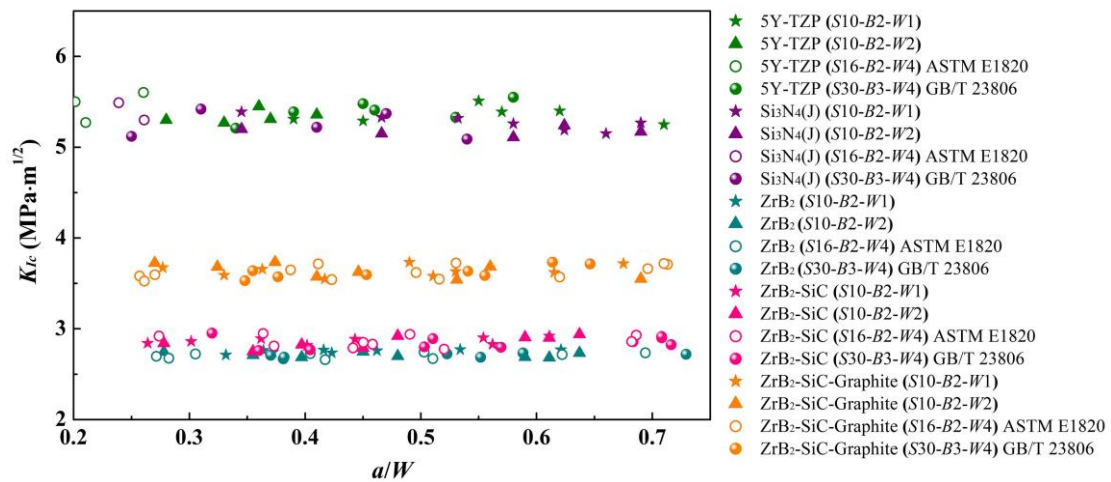


Fig. 10. Experiment results of sample size effect on the measurement of fracture toughness in 5Y-TZP,  $\text{Si}_3\text{N}_4(\text{J})$ ,  $\text{ZrB}_2$ ,  $\text{ZrB}_2\text{-SiC}$  and  $\text{ZrB}_2\text{-SiC-Graphite}$  ceramics.

#### 4. Conclusions

In order to promote the standardization of laser notching method, in this work, the effects of laser notch tip radius ( $\rho$ ), notch depth ( $a$ ), equivalent notch angle ( $\theta$ ) and

sample size on the measured value of fracture toughness ( $K_{Ic}$ ) were systematically studied. Following are the main conclusions:

(1) The laser notching method is a very versatile method, which seems to be applicable to all ceramic materials (including oxide, nitride, carbide and boride ceramics). The V-notch tip radius prepared by laser method can be easily lower than 1  $\mu\text{m}$ , which is one order of magnitude lower than the traditional methods.

(2) In double logarithmic coordinates, the  $K_{Ic}$  value almost increases linearly when the  $\rho$  exceeds the critical notch tip radius ( $\rho_c$ ), namely, the  $K_{Ic}$  value is proportional to  $\rho^n$ , where  $n$  is normally in the range of 0.1-0.5 depending on the material itself. For fine-grained ceramics with submicron grain size (3Y-TZP and 5Y-TZP), the critical tip radius ( $>5 \mu\text{m}$ ) is still far from reaching the limit of laser notching method.

(3) For monolithic ceramics, the  $K_{Ic}$  value will reach a plateau when the relative notch depth ( $a/W$ ) exceeds 0.15, which is much lower than 0.35 that is recommended in existing standards.

(4) The relationship between the  $K_{Ic}$  value and  $\theta$  in ceramics follows well with the GÓMEZ criterion, that is, the  $\theta$  should be at least less than  $60^\circ$  in order to avoid overestimation of  $K_{Ic}$ . Considering that it is challenging to perfectly overlap the V-notch and the U-groove during processing, which inevitably leads to poor consistency and overestimation of measured values of  $K_{Ic}$ , it could be more reasonable to refer to the requirement given by ISO 23146-2012 ( $\theta < 30^\circ$ ).

(5) The SEVNB technique combined with laser notching method can be applicable to various ceramic small and thin plates with thickness from 1 to 2 mm.

Accordingly, it is safe to conclude that fracture toughness can be accurately measured by using small specimens with the thickness of less than 2mm in conjunction with the laser direct-notching method. In this case, the outstanding advantages of the laser method, such as fast, good efficiency, low cost as well as low material consumption, can be fully exploited.

### **Acknowledgement**

Financial support was provided by the Natural Science Foundation of Jiangsu

Province (No. BK20201040), the Surface Projects of Natural Science Research in Jiangsu Province (No. 19KJB430021), the Special Talent Introduction for “Double Innovation Plan” in 2019, the University Research Foundation of Nanjing Institute of Technology (No. YKJ201806), the National Natural Science Foundation of China (No. 52002108), the Natural Science Foundation of Hebei Province (No. E2020202002) and the Outstanding Scientific and Technological Innovation Team in Colleges and Universities of Jiangsu Province.

## References

- [1] J. Lamon, 1-Flaws in materials, Brittle fracture and damage of structural ceramics & composites, 2016, 1-33.
- [2] A.G. Evans, Fracture Mechanics Determinations, Concepts, Flaws, and Fractography, Springer, US, 1974.
- [3] ASTM-C-1421, Standard test methods for determination of fracture toughness of advanced ceramics at ambient temperature. ASTM-C-1421; 2016.
- [4] ASTM E1820-13, Standard test method for measurement of fracture toughness. 2014.
- [5] ASTM E1290-08, Standard test method for crack-tip opening displacement (CTOD) fracture toughness measurement. West Conshohocken: American Society for Testing and Materials; 2008.
- [6] ISO-15732, Fine ceramics (advanced ceramics, advanced technical ceramics)—test method for fracture toughness of monolithic ceramics at room temperature by single edge precracked beam (SEPB) method; 2003.
- [7] ISO-24370, Test method for fracture toughness of monolithic ceramics at room temperature by chevron-notched beam(CNB) method; 2005.
- [8] ISO-23146, Test methods for fracture toughness of monolithic ceramics—single-edge V-notch beam (SEVNB) method; 2012.
- [9] GB/T 23806-2009, General administration of quality supervision, inspection and quarantine of the People’s Republic of China, Standardization Administration of the People’s Republic of China. Fine Ceramics (Advanced Ceramics, Advanced Technical Ceramics)-test method for fracture toughness of monolithic ceramics at

room temperature by single edge precracked beam (SEPB) method (China Standard GB/T 23806-2009), 2009.

- [10] DIN EN 14425-3, Advanced technical ceramics—test methods for determination of fracture toughness of monolithic ceramics—Part 3: chevron notched beam (CNB) method.
- [11] A.Z. Wang, B. Du, P. Hu, *et al.*, Reliable evaluation of fracture toughness in ceramics via nanosecond laser notching method, *J. Eur. Ceram. Soc.* 39 (2019) 883-889.
- [12] T. Nose, T. Fujii, Evaluation of fracture toughness for ceramic materials by a single-edge-precracked-beam method, *J. Am. Ceram. Soc.* 71 (2010) 328-333.
- [13] D. Munz, R.T. Bubsey, J.E. Srawley, Compliance and stress intensity coefficients for short bar specimens with chevron notches, *Int. J. Fracture.* 16 (1980) 359-374.
- [14] C. Tracy, G. Quinn, Fracture toughness by the surface crack in flexure (SCF) method, *Ceram. Eng. and Sci. Proc.* 15 (1994) 837-845.
- [15] G.M. Song, Y. Zhou, Y. Sun, Modeling of fiber toughening in fiber-reinforced ceramic composites, *Ceram. Int.* 25 (1999) 257-260.
- [16] P.F. Cesar, A. Della Bona, S.S. Scherrer, *et al.*, ADM guidance—Ceramics: Fracture toughness testing and method selection, *Dent. Mater.* 33 (2017) 575-584.
- [17] H.D. Carlton, J.W. Elmer, D.C. Freeman, *et al.*, Laser notching ceramics for reliable fracture toughness testing, *J. Eur. Ceram. Soc.* 36 (2016) 227-234.
- [18] M. Sakai, R.C. Bradt, Fracture toughness testing of brittle materials, *Int. Mater. Rev.* 38 (1993) 53-78.
- [19] I. Bar-On, J.T. Beals, G.L. Leatherman, *et al.*, Fracture toughness of ceramic precracked bend bars, *J. Am. Ceram. Soc.* 73 (1990) 2519-2522.
- [20] T. Nishida, T. Shiono, T. Nishikawa, On the fracture toughness of polycrystalline alumina measured by SEPB methods, *J. Eur. Ceram. Soc.* 5 (1989) 379-383.

- [21]R. Belli, M. Wendler, J. Zorzin, *et al.*, Fracture toughness mode mixity at the connectors of monolithic 3Y-TZP and LS2 dental bridge constructs, *J. Eur. Ceram. Soc.* 35 (2015) 3701-3711.
- [22]H. Fischer, A. Waindich, R. Telle, Influence of preparation of ceramic SEVNB specimens on fracture toughness testing results, *Dent. Mater.* 24 (2008) 618-622.
- [23]J. Rodríguez, A. Salazar, F.J. Gómez, *et al.*, Fracture of notched samples in epoxy resin: Experiments and cohesive model, *Eng. Fract. Mech.* 149 (2015) 402-411.
- [24]H. Awaji, Y. Sakaida, V-notch technique for single-edge notched beam and chevron notch methods, *J. Am. Ceram. Soc.* 73 (1990) 3522-3523.
- [25]T. Fett, Influence of a finite notch root radius on fracture toughness, *J. Eur. Ceram. Soc.* 25 (2005) 543-547.
- [26]A.Z. Wang, P. Hu, X.H. Zhang, *et al.*, Accurate measurement of fracture toughness in structural ceramics, *J. Eur. Ceram. Soc.* 37 (2017) 4207-4212.
- [27]H.D. Carlton, J.W. Elmer, D.C. Freeman, *et al.*, Laser notching ceramics for reliable fracture toughness testing, *J. Eur. Ceram. Soc.* 36 (2016) 227-234.
- [28]W. Zhao, P. Rao, Z. Ling, A new method for the preparation of ultra-sharp V-notches to measure fracture toughness in ceramics, *J. Eur. Ceram. Soc.* 34 (2014) 4059-4062.
- [29]M. Turon-Vinas, M. Anglada, Assessment in  $\text{Si}_3\text{N}_4$  of a new method for determining the fracture toughness from a surface notch micro-machined by ultra-short pulsed laser ablation, *J. Eur. Ceram. Soc.* 35 (2015) 1737-1741.
- [30]A.Z. Wang, P. Hu, X.Y. Zhao, *et al.*, Modelling and experimental investigation of pore-like flaw-strength response in structural ceramics, *Ceram. Int.* 46 (2020) 14431-14438.
- [31]W. Zhao, J.P. Cui, P.G. Rao, Effect of molten zone ablated by femtosecond laser on fracture toughness of  $\text{Si}_3\text{N}_4$  measured by SEVNB method, *J. Eur. Ceram. Soc.* 38 (2018) 2243-2246.

- [32] J.P. Cui, Z.Y. Gong, P.G. Rao, Effect of molten zone ablated by femtosecond laser on fracture toughness of oxide ceramics, *J. Eur. Ceram. Soc.* 38 (2018) 2440-2444.
- [33] W. Zhao, J.P. Cui, P.G. Rao, Effect of thermal stress induced by femtosecond laser on fracture toughness of fine-grained alumina, *J. Aust. Ceram. Soc.* 55 (2019) 575-578.
- [34] D. Munz, T. Fett, *Ceramics: mechanical properties, failure behaviour, materials selection*. 1st ed. Berlin, Heidelberg: Springer-Verlag; 1999.
- [35] S.S. Scherrer, I.L. Denry, H.W. Anselm Wiskott, Comparison of three fracture toughness testing techniques using a dental glass and a dental ceramic, *Dent. Mater.* 14 (1998) 246-255.
- [36] R. Damani, R. Gstrein, R. Danzer, Critical notch-root radius effect in SENB-S fracture toughness testing, *J. Eur. Ceram. Soc.* 16 (1996) 695-702.
- [37] J.M. Alkin, A.S. Tetelman, Relation between  $K_{Ic}$  and microscopic strength for low alloy steels, *Eng. Fract. Mech.* 3 (1971) 151-167.
- [38] T. Nishida, Y. Hanaki, Effect of notch-root radius on the fracture toughness of a fine-grained alumina, *J. Am. Ceram. Soc.* 77 (1994) 606-608.
- [39] D. Taylor, P. Cornetti, N. Pugno, The fracture mechanics of finite crack extension, *Eng. Fract. Mech.* 72 (2005) 1021-1038.
- [40] X.H. Zhang, P. Hu, J.C. Han, *et al.*, Study on thermal shock resistance and oxidation resistance of ultra-high temperature ceramics, *Mater. China.* 30 (2011) 27-31.
- [41] R.W. Steinbrech, A. Reichl, W. Schaarwächter, R-curve behavior of long cracks in alumina, *J. Am. Ceram. Soc.* 73 (1990) 2009-2015.
- [42] Y. Torres, R. Bermejo, L. Llanes, *et al.*, Influence of notch radius and R-curve behaviour on the fracture toughness evaluation of WC-Co cemented carbides, *Eng. Fract. Mech.* 75 (2008) 4422-4430.
- [43] R.O. Ritchie, The conflicts between strength and toughness, *Nat. Mater.* 10 (2011) 817-822.
- [44] M.S. Asl, I. Farahbakhsh, B. Nayebi, Characteristics of multi-walled carbon

- nanotube toughened ZrB<sub>2</sub>-SiC ceramic composite prepared by hot pressing, *Ceram. Int.* 42 (2016) 1950-1958.
- [45] H.Y. Xing, B. Zou, S.S. Li, *et al.*, Study on surface quality, precision and mechanical properties of 3D printed ZrO<sub>2</sub> ceramic components by laser scanning stereolithography, *Ceram. Int.* 43 (2017) 16340-16347.
- [46] D.T. Jiang, O. VanderBiest, J. Vleugels, ZrO<sub>2</sub>-WC nanocomposites with superior properties, *J. Eur. Ceram. Soc.* 27 (2007) 1247-1251.
- [47] D.K. Shetty, A.R. Rosenfield, W.H. Duckworth, *et al.*, A biaxial-flexure test for evaluating ceramic strengths, *J. Am. Ceram. Soc.* 66 (1983) 36-42.
- [48] J. Watts, G. Hilmas, W.G. Fahrenholtz, Mechanical characterization of ZrB<sub>2</sub>-SiC composites with varying SiC particle sizes, *J. Am. Ceram. Soc.* 94 (2011) 4410-4418.
- [49] A.G. Evans, J.M. Domergue, E. Vagaggini, Methodology for relating the tensile constitutive behavior of ceramic-matrix composites to constituent properties, *J. Am. Ceram. Soc.* 77 (1994) 1425-1435.
- [50] J. Wang, W.M. Rainforth, I. Wadsworth, *et al.*, The effects of notch width on the SENB toughness for oxide ceramics, *J. Eur. Ceram. Soc.* 10 (1992) 21-31.
- [51] G.A. Gogotsi, Fracture toughness of ceramics and ceramic composites, *Ceram. Int.* 29 (2003) 777-784.
- [52] K. Ando, M. Iwasa, B.A. Kim, *et al.*, Effects of crack length, notch root radius and grain size on fracture toughness of fine ceramics, *Fatigue. Fract. Eng. M.* 16 (1993) 995-1006.
- [53] K. Tsuji, K. Iwase, K. Ando, An investigation into the location of crack initiation sites in alumina, polycarbonate and mild steel, *Fatigue. Fract. Eng. M.* 22 (1999) 509-517.
- [54] R.L. Bertolotti, Fracture toughness of polycrystalline Al<sub>2</sub>O<sub>3</sub>, *J. Am. Ceram. Soc.* 56 (1973) 107.
- [55] W. Tang, Y.W. Shi, Influence of strength matching and crack depth on fracture toughness of welded joints, *Eng. Fract. Mech.* 51 (1995) 649-659.
- [56] W. Zhao, C. Peng, M. Lv, *et al.*, Effect of notch depth on fracture toughness of

- Y-TZP and determination of its actual value, *Ceram. Int.* 41 (2015) 869-872.
- [57] A.Z. Wang, Y.Z. Wang, C. Zhang, *et al.*, On the estimation and modeling of fracture toughness in structural ceramics in a simple way, *Theor. Appl. Fract. Mech.* 103 (2019) 102273.
- [58] M. Turon-Vinas, M. Anglada, Fracture toughness of zirconia from a shallow notch produced by ultra-short pulsed laser ablation, *J. Eur. Ceram. Soc.* 34 (2014) 3865-3870.
- [59] M. Turon-Vinas, J. Morillas, P. Moreno, M. Anglada, Evaluation of damage in front of starting notches induced by ultra-short pulsed laser ablation for the determination of fracture toughness in zirconia, *J. Eur. Ceram. Soc.* 37 (2017) 5127-5131.
- [60] N. Ramachandran, D.K. Shetty, Rising crack-growth-resistance (R-curve) behavior of toughened alumina and silicon nitride, *J. Am. Ceram. Soc.* 74 (1991) 2634-2641.
- [61] H.J. Choi, K.S. Cho, L.G. Lee, *et al.*, R-curve behavior of silicon nitride-titanium nitride composites, *J. Am. Ceram. Soc.* 80 (1997) 2681-2684.
- [62] A.Z. Wang, B. Du, P. Hu, *et al.*, Accurate evaluation of critical flaw size in structural ceramics via femtosecond laser, *Ceram. Int.* 2018, 44(18): 23008-23013.
- [63] A. Paskin, G.J. Dienes, Molecular dynamic simulations of shock waves in a three-dimensional solid, *J. Appl. Phys.* 43 (1972) 1605-1610.
- [64] M.A. Meyers, J. McKittrick, P.Y. Chen, Structural biological materials: critical mechanics-materials connections, *Science* 339 (2013) 773-779.
- [65] F. Kern, R. Gadow, Alumina toughened zirconia from yttria coated powders, *J. Eur. Ceram. Soc.* 32 (2012) 3911-3918.
- [66] C. Wu, Y.K. Li, C.L. Wan, Reactive-sintering B<sub>4</sub>C matrix composite for armor applications, *Rare. Met.* 39 (2020) 529-544.
- [67] M.Y. Xiu, Q.L. Han, J.L. Xue, *et al.*, Effect of carbon source and adding ratio on the microstructure and properties of solid-state sintering silicon carbide, *J. Inorg. Mater.* 28 (2013) 1009-1013.

- [68] W.C. Oliver, C.J. McHargue, Characterizing the hardness and modulus of thin films using a mechanical properties microprobe, *Thin. Solid. Films.* 161 (1988) 117-122.
- [69] X.H. Zhang, X.G. Luo, J.P. Li, *et al.*, The ideal strength of transition metal diborides  $TMB_2$  (TM=Ti, Zr, Hf): Plastic anisotropy and the role of prismatic slip, *Scripta. Mater.* 62 (2010) 625-628.
- [70] F.J. Gómez, M. Elices, A fracture criterion for sharp V-notched samples, *Int. J. Fracture.* 123 (2003) 163-175.
- [71] H. Miyazaki, Y.I. Yoshizawa, K. Hirao, *et al.*, Measurements of fracture toughness of ceramic thin plates through single-edge V-notch plate method, *J. Eur. Ceram. Soc.* 36 (2016) 4327-4331.

# Figures

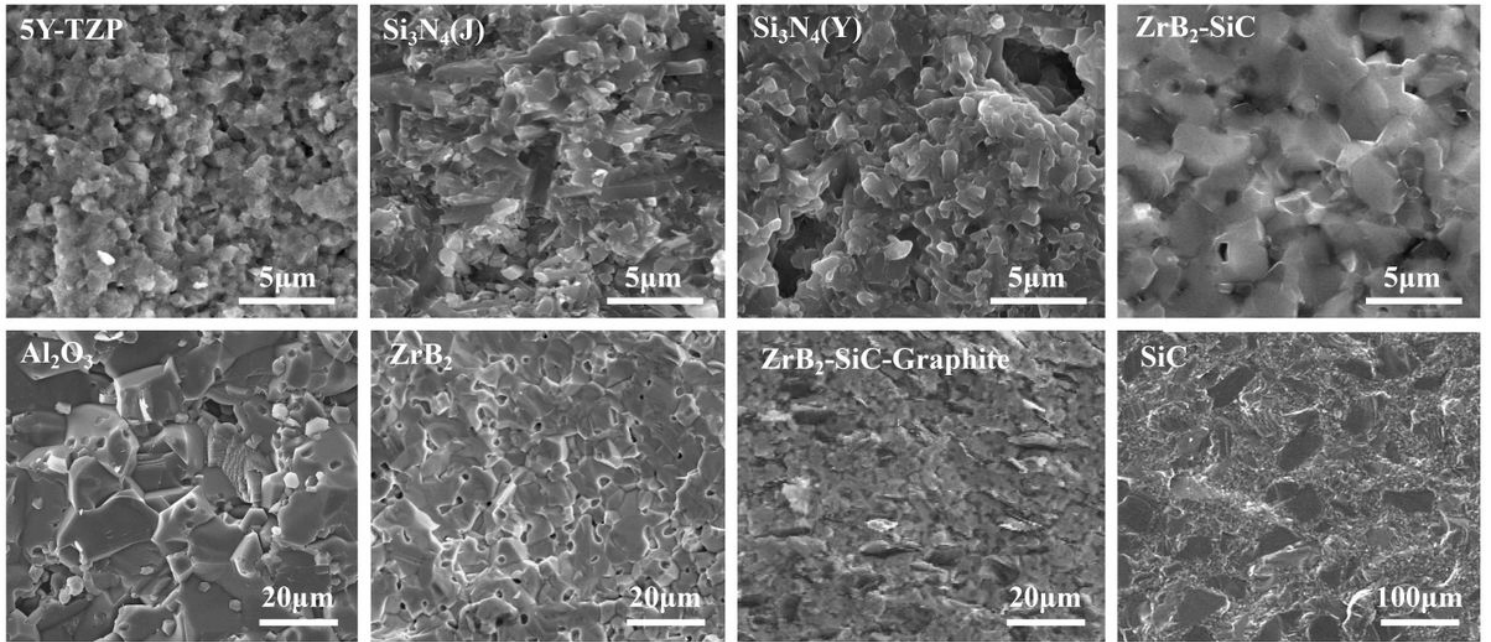
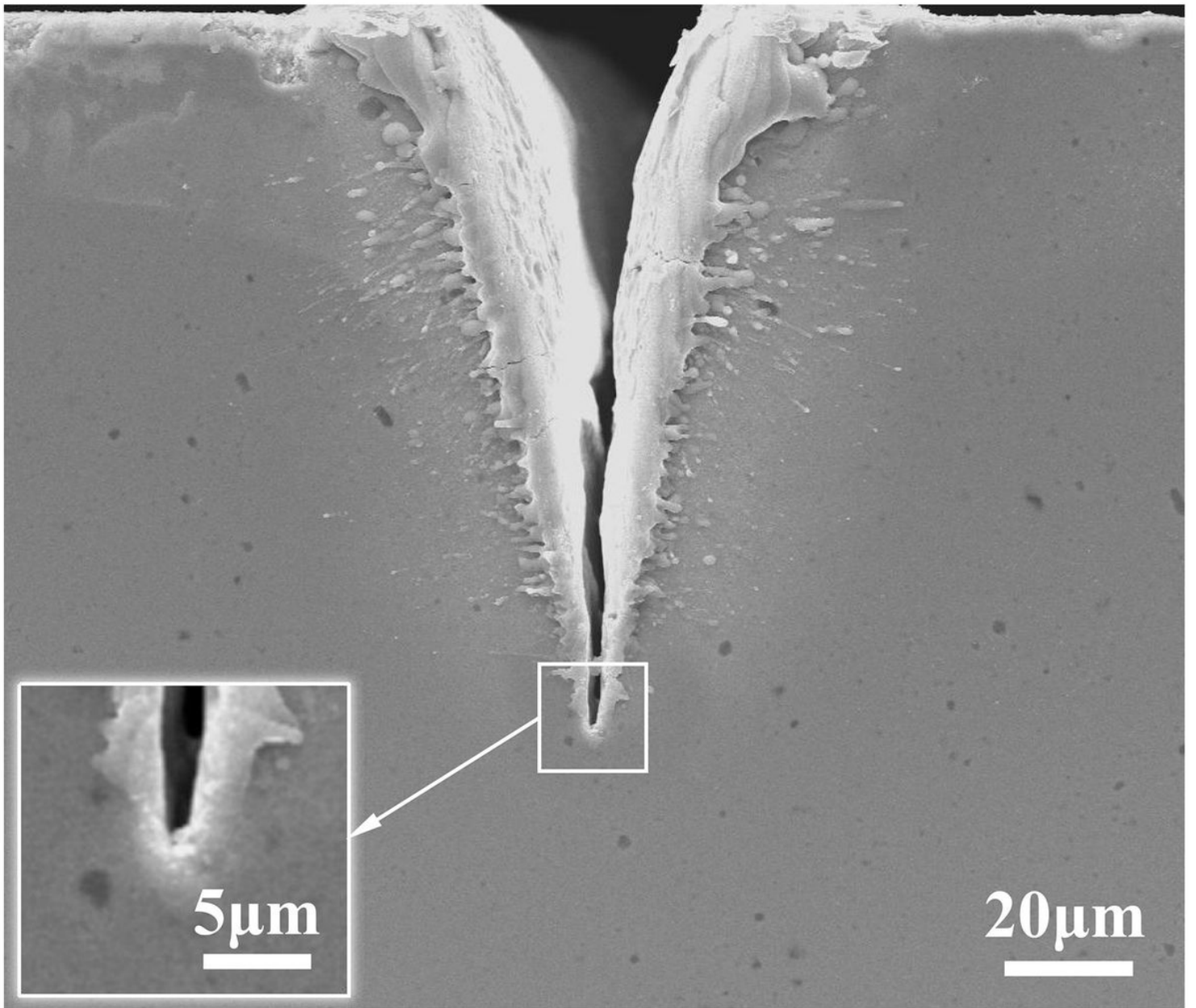


Figure 1

SEM images of fracture surfaces of test samples.



**Figure 2**

SEM image of 5Y-TZP ceramic bar with an ultra-sharp V-notch. The enlarged view shows that the V-notch tip radius is  $\sim 0.7 \mu\text{m}$  and no microcrack is found near the V-notch root.

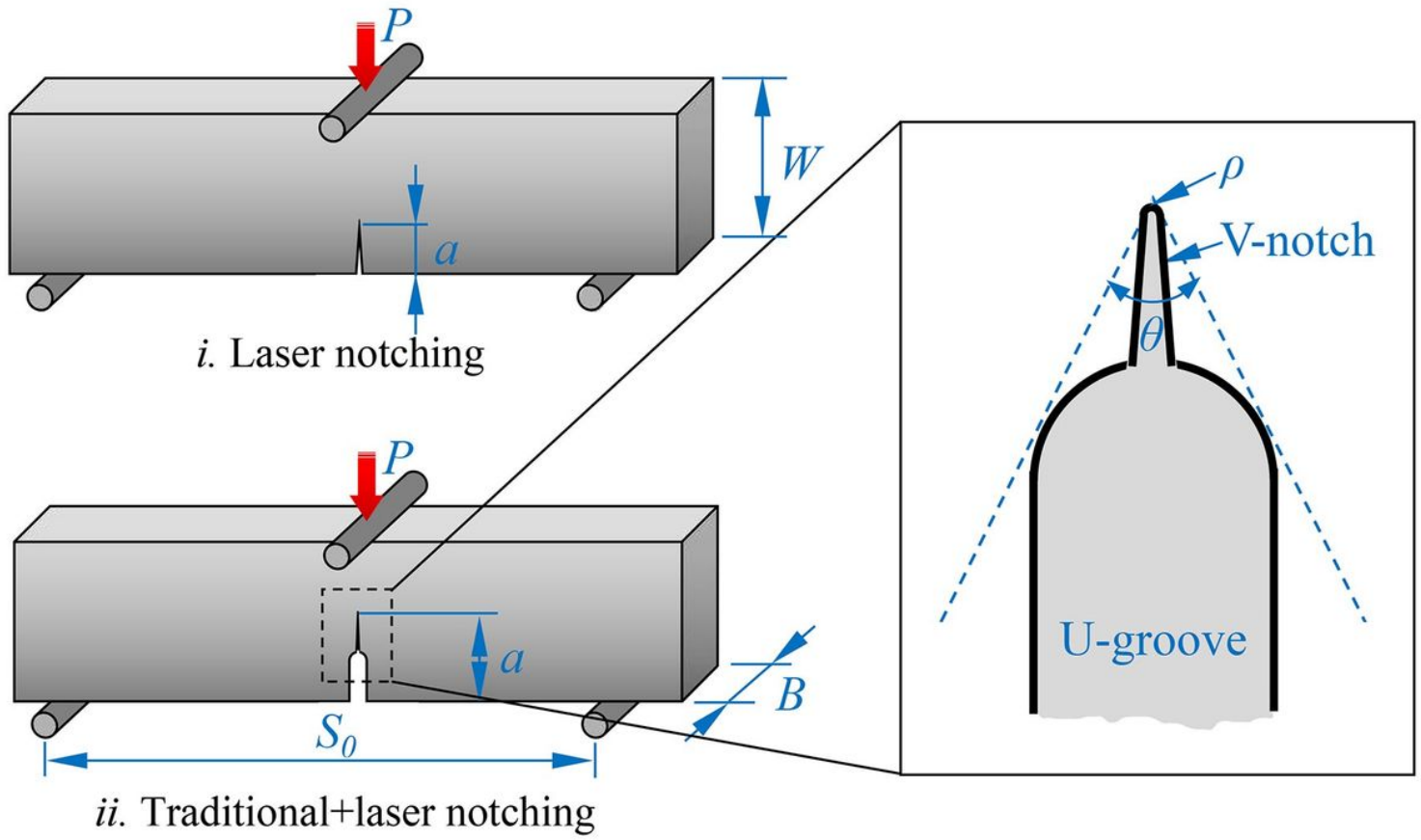


**Figure 3**

Schematic of the SEVNB test specimens with sharp notches.

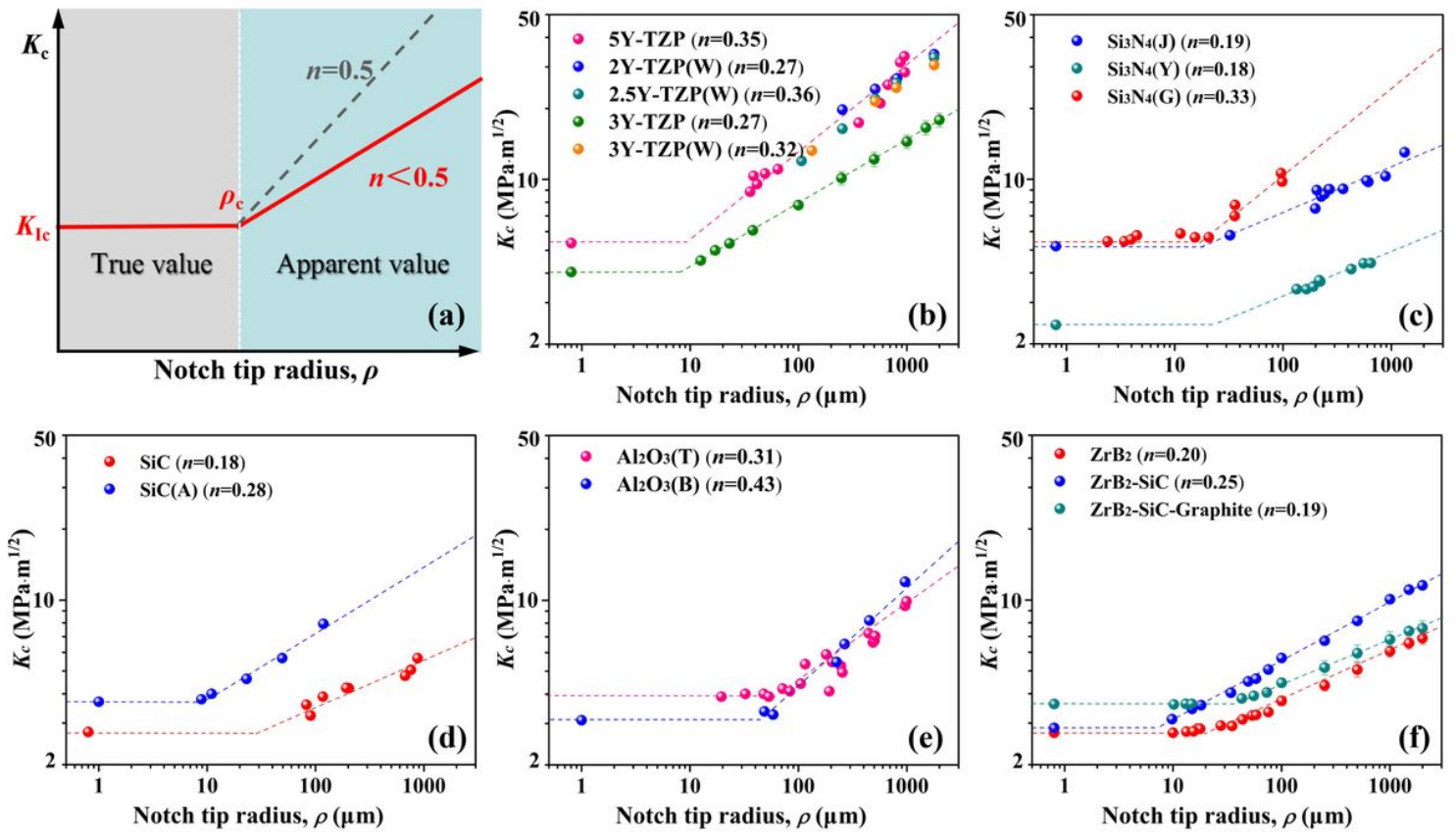


**Figure 4**

Variation of the critical stress intensity factor ( $K_c$ ) with notch tip radius ( $\rho$ ). (a) Schematic diagram and test results of (b) yttria-stabilized zirconia, (c) silicon nitride, (d) silicon carbide, (e) alumina as well as (f) ZrB<sub>2</sub>-based ceramics in double logarithmic coordinates.

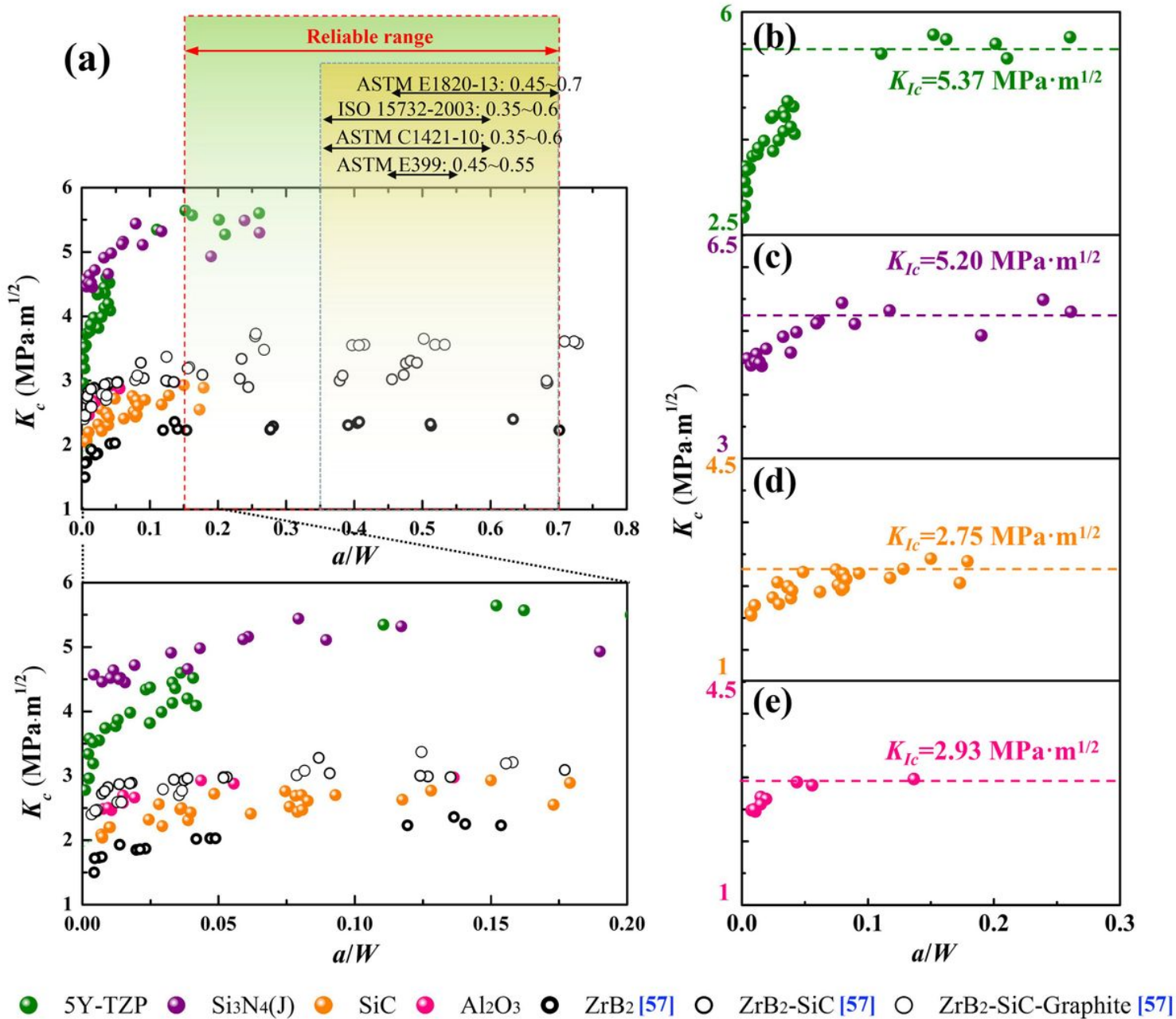


Figure 5

Fracture toughness of various ceramics with different  $a/W$  measured by laser notched SEVNB method. (a) Our work and the literature report data [57] and (b) 5Y-TZP, (c) Si<sub>3</sub>N<sub>4</sub>(J), (d) SiC as well as (e) Al<sub>2</sub>O<sub>3</sub> ceramics, respectively.

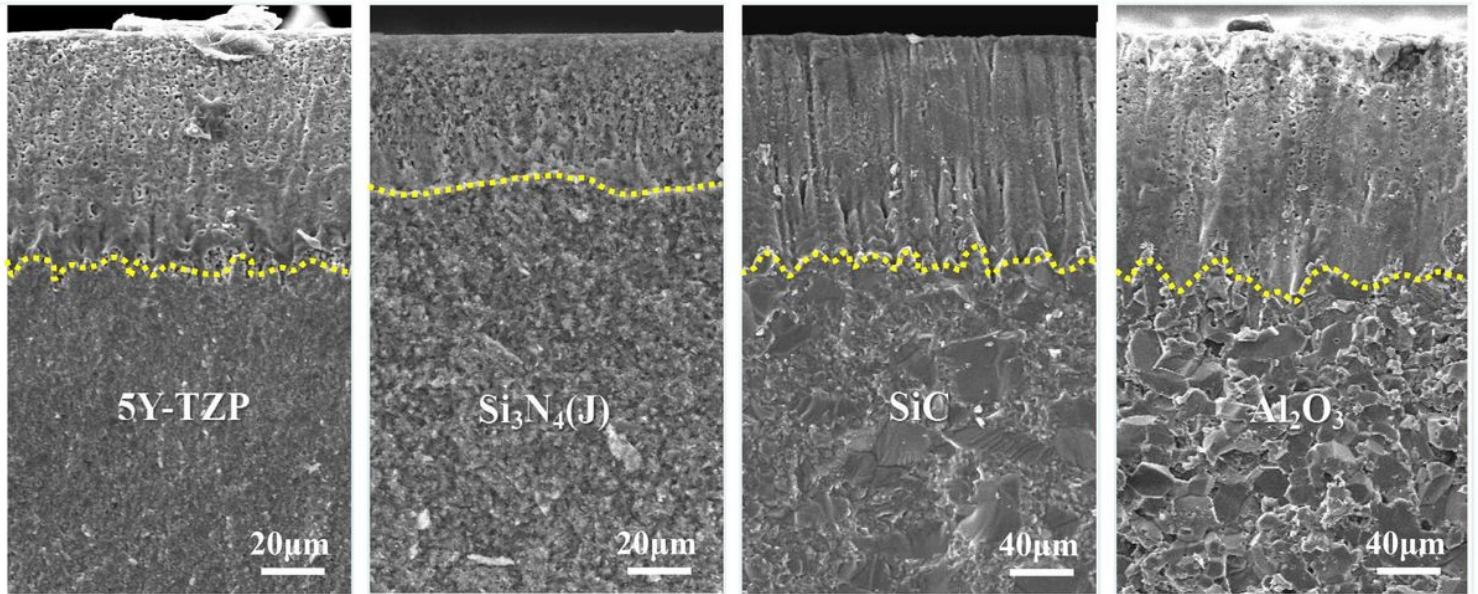


Figure 6

Fracture surfaces of test ceramics notched by nanosecond laser.

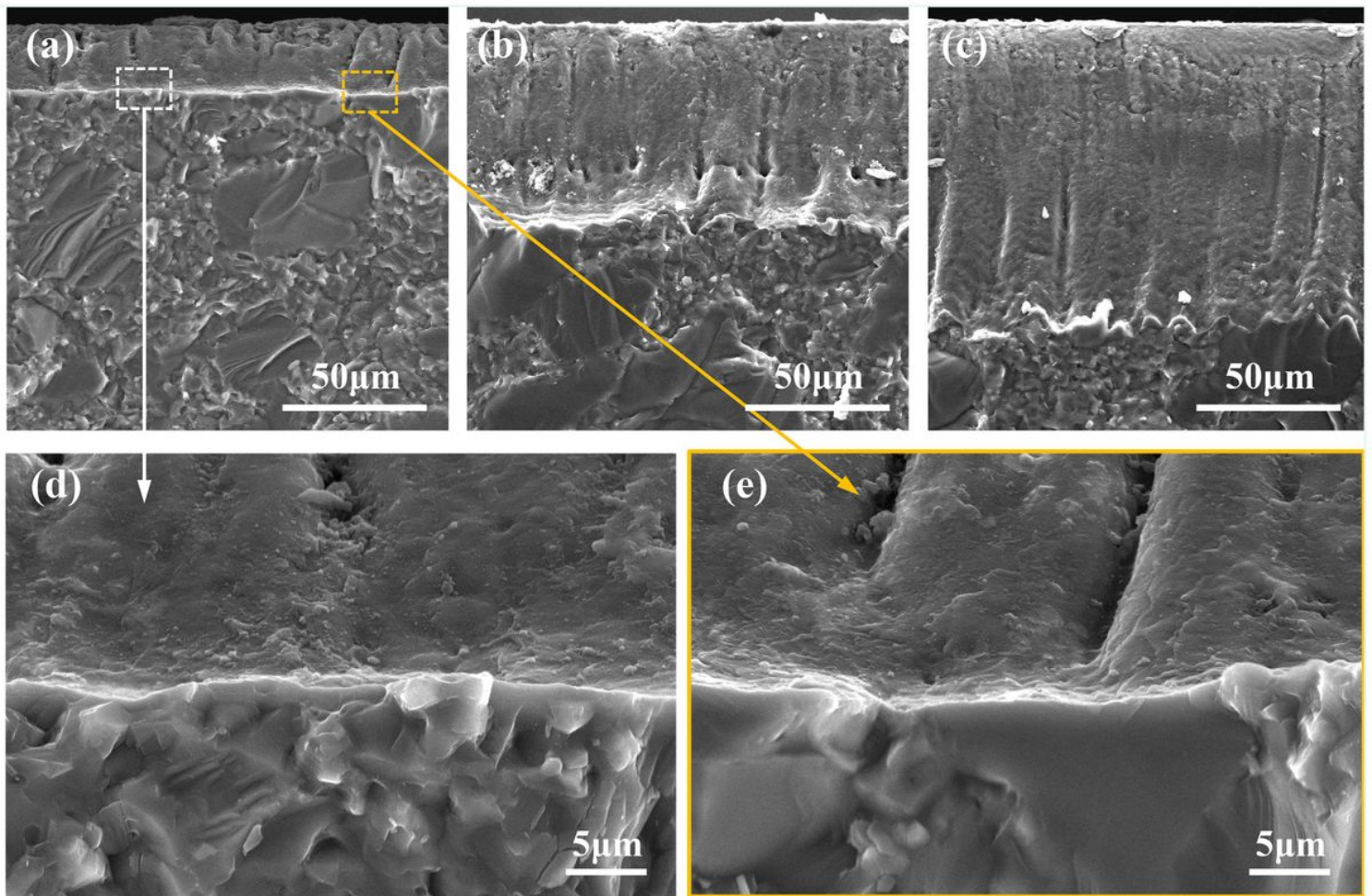


Figure 7

Fracture surfaces of SiC ceramic with various notch depth.

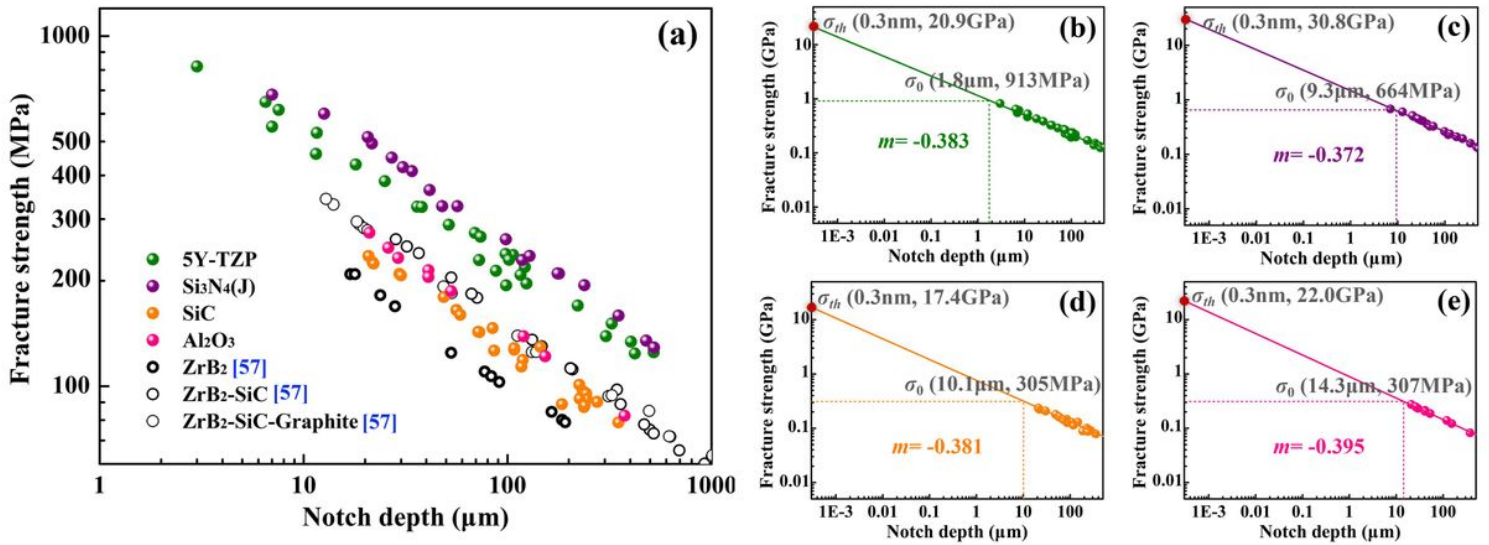
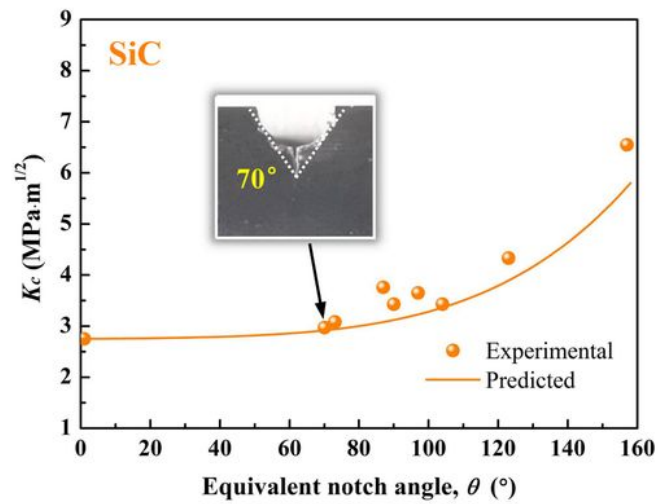
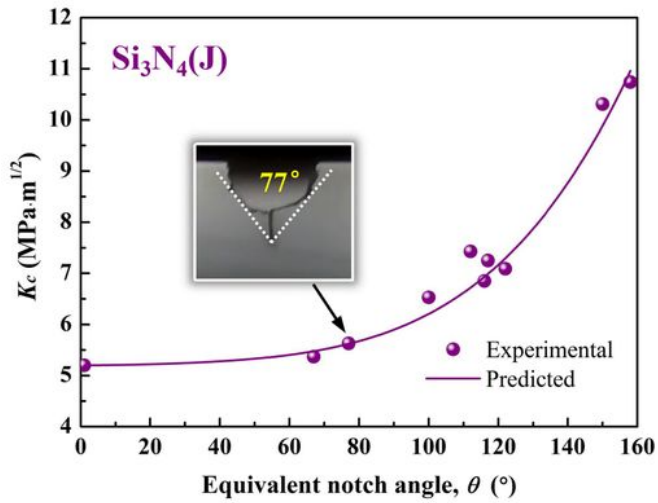
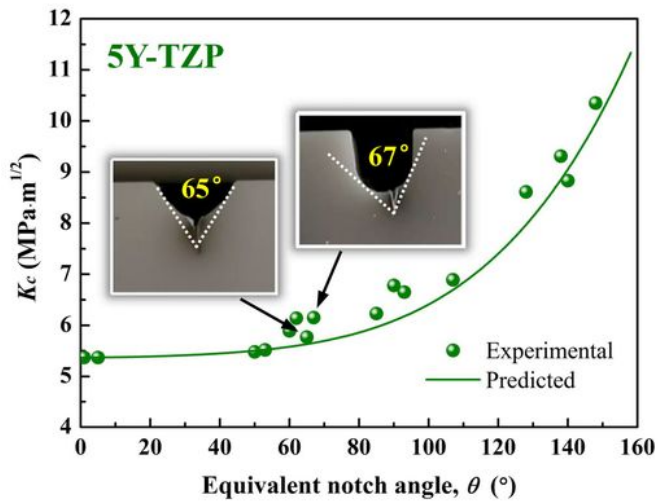


Figure 8

Relationship between fracture strength and notch depth for various ceramics in double logarithmic coordinates. (a) Our work and the literature report data [57] and (b) 5Y-TZP, (c)  $\text{Si}_3\text{N}_4(\text{J})$ , (d) SiC as well as (e)  $\text{Al}_2\text{O}_3$  ceramics, respectively.



**Figure 9**

Experimental and predicted values of  $K_c$  in 5Y-TZP, Si<sub>3</sub>N<sub>4</sub>(J) and SiC samples with various equivalent notch angles ( $\theta$ ).

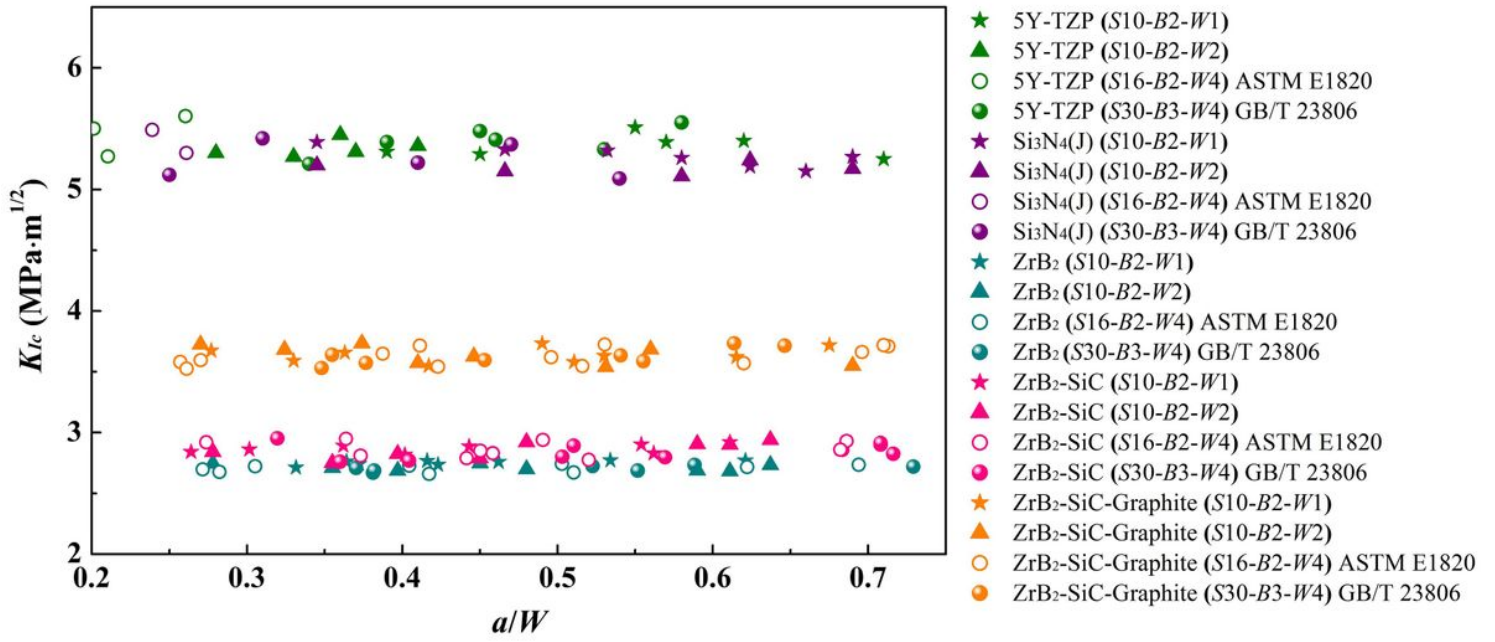


Figure 10

Experiment results of sample size effect on the measurement of fracture toughness in 5Y-TZP, Si<sub>3</sub>N<sub>4</sub>(J), ZrB<sub>2</sub>, ZrB<sub>2</sub>-SiC and ZrB<sub>2</sub>-SiC-Graphite ceramics.